AD-A182 838 UNIFIED REAL PART OF THE SUSCEPTIBILITY FOR COLLISIONAL BROADENING..(U) PENNSYLVANIA STATE UNIV UNIVERSITY PARK DEPT OF ELECRRICAL EN.. KTTOMIYAMA ET AL. 15 AUG 86 1/1

UNCLASSIFIED AFGL-TR-86-0181 F49620-82-C-0035 F/G 20/5 NL

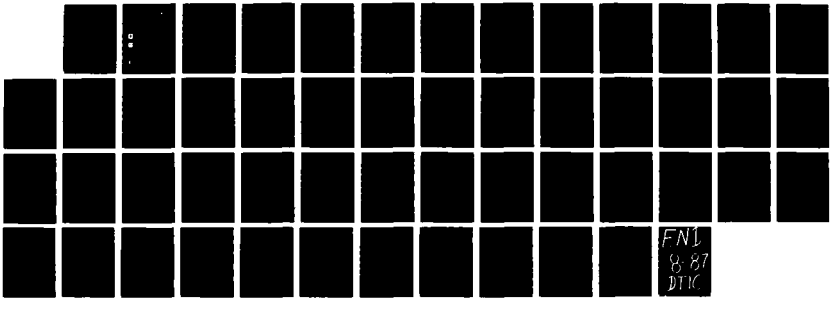

FNL
8-87
DTIC

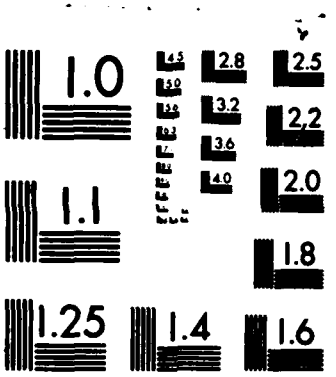

AFGL-TR-86-0181
ENVIRONMENTAL RESEARCH PAPERS, NO. 961

Unified Real Part of the Susceptibility for Collisional Broadening

K. TOMIYAMA
S. A. CLOUGH
F. X. KNEIZYS

15 August 1986

OPTICAL PHYSICS DIVISION
PROJECT 2310
AIR FORCE GEOPHYSICS LABORATORY
HANSCOM AFB, MA 01731

Unclassified

SECURITY CLASSIFICATION OF THIS PAGE

REPORT DOCUMENTATION PAGE

1a. REPORT SECURITY CLASSIFICATION UNCLASSIFIED	1b. RESTRICTIVE MARKINGS
2a. SECURITY CLASSIFICATION AUTHORITY	3. DISTRIBUTION / AVAILABILITY OF REPORT Approved for public release; Distribution unlimited
2b. DECLASSIFICATION / DOWNGRADING SCHEDULE	
4. PERFORMING ORGANIZATION REPORT NUMBER(S) AFGL-TR-86-0181 ERP, No. 961	5. MONITORING ORGANIZATION REPORT NUMBER(S)
6a. NAME OF PERFORMING ORGANIZATION Air Force Geophysics Laboratory 6b. OFFICE SYMBOL (If applicable) OPI	7a. NAME OF MONITORING ORGANIZATION
6c. ADDRESS (City, State, and ZIP Code) Hanscom AFB Massachusetts 01731	7b. ADDRESS (City, State, and ZIP Code)
8a. NAME OF FUNDING / SPONSORING ORGANIZATION 8b. OFFICE SYMBOL (If applicable)	9. PROCUREMENT INSTRUMENT IDENTIFICATION NUMBER
8c. ADDRESS (City, State, and ZIP Code)	10. SOURCE OF FUNDING NUMBERS PROGRAM ELEMENT NO. 61102F; PROJECT NO. 2310; TASK NO. 2310G1; WORK UNIT ACCESSION NO. 2310G110

11. TITLE (Include Security Classification)
Unified Real Part of the Susceptibility for Collisional Broadening

12. PERSONAL AUTHOR(S)
*K. Tomiyama, S.A. Clough and F.X. Kneizys

13a. TYPE OF REPORT	13b. TIME COVERED	14. DATE OF REPORT (Year, Month, Day)	15. PAGE COUNT
Scientific Interim	FROM _____ TO _____	1986 August 15	54

16. SUPPLEMENTARY NOTATION
*The Pennsylvania State University, The Department of Electrical Engineering, University Park, PA 16802

17. COSATI CODES		
FIELD	GROUP	SUB-GROUP

18. SUBJECT TERMS (Continue on reverse if necessary and identify by block number)
Real Susceptibility

19. ABSTRACT (Continue on reverse if necessary and identify by block number)

As a consequence of the extensive study of the emission and absorption of spectral radiation, significant advances have been made in the understanding of the imaginary part of the susceptibility for collisionally broadened transitions. An absorption line shape in the impact approximation has been developed which is applicable from the microwave through the infrared and for which a first order treatment of line coupling is available. In this report we develop the real part of the susceptibility, applicable to the computation of the complex index of refraction and propagation delays, which is associated with this absorption line shape. The approach is to examine the two extreme cases of the millimeter and infrared regions, obtained through the Hilbert transform (the Kramers-Kronig relationship) and the respective approximate imaginary parts. The two limiting forms suggest a unified approximate formulation for the real part of susceptibility. The proposed analytical formulation is numerically compared with the exact result using a newly obtained expression for the exact real part.

20. DISTRIBUTION / AVAILABILITY OF ABSTRACT ☒ UNCLASSIFIED/UNLIMITED ☒ SAME AS RPT. ☐ DTIC USERS	21. ABSTRACT SECURITY CLASSIFICATION UNCLASSIFIED
22a. NAME OF RESPONSIBLE INDIVIDUAL Shepard A. Clough	22b. TELEPHONE (Include Area Code) (617) 377-2337 22c. OFFICE SYMBOL OPI

DD FORM 1473, 84 MAR 83 APR edition may be used until exhausted. All other editions are obsolete.

SECURITY CLASSIFICATION OF THIS PAGE
Unclassified

Preface

The major part of this study was carried out during the first author's stay at the Air Force Geophysics Laboratory (AFGL), Hanscom Air Force Base, Mass., in the summer of 1984, as a fellow of the Summer Faculty Research Program of the Southeast Center for Electrical Engineering Education sponsored by the Air Force Systems Command, Air Force Office of Scientific Research (AFOSR), United States Air Force, under Contract F49620-82-C-0035. Helpful discussions with Dr. D.R. Brown of the Atmospheric Sciences Laboratory, White Sands Missile Range, United States Army are also acknowledged. Finally, Dr. Tomiyama acknowledges the contribution of John Piorkowski in the computational aspects of this study.

A-1

Contents

Illustrations

Tables

Unified Real Part of the Susceptibility for Collisional Broadening

1. INTRODUCTION

As a consequence of the extensive study of the emission and absorption of spectral radiation, significant advances have been made in the understanding of the imaginary part of the susceptibility for collisionally broadened transitions.[1-4] An absorption line shape in the impact approximation has been developed that is applicable from the microwave through the infrared and for which a first order treatment of line coupling is available. In this report we develop the real part of the susceptibility, applicable to the computation of the index of refraction and propagation delays, which is associated with this absorption line shape.

(Received for publication 12 August 1986)

1. Clough, S.A., Davies, R.W., and Tipping, R.H. (1983) The line shape for collisionally broadened molecular transitions: a quantum theory satisfying the fluctuation dissipation theorem, in Spectral Line Shape Vol. 2, edited by K. Burnett, Walter de Gruyter, New York, NY, 1983, pp 553-568.

2. Liebe, H.J. (1981) Modeling attenuation and phase of radio waves in air at frequencies below 1000 GHz, Radio Science, 16, No. 6:1183-1199.

3. Kemp, A.J., Birch, J.R., and Afsar, M.N. (1978) The refractive index of water vapor: a comparison of measurement and theory, Infrared Physics, 18:827-833.

4. Marshall, A.G., and Roe, D.C. (1978) Dispersion versus absorption: spectral line shape analysis for radiofrequency and microwave spectrometry, Analyt. Chem., 50, No. 6:756-763.

The complex susceptibility, χ , characterizes the linear relationship between the polarization, P, and the impressed field, $E = E_0 \exp(i2\pi c \nu t)$, through the expression

$$P = \chi(\nu)\, E_0 \exp(i2\pi c \nu t), \tag{1.1}$$

where ν is the wavenumber value and c is the velocity of light. The susceptibility is expressed in terms of its real and imaginary parts as

$$\chi(\nu) = \chi'(\nu) - i\,\chi''(\nu). \tag{1.2}$$

For a plane wave propagating in the z direction through a nonmagnetic dielectric medium (permeability = 1) with complex index of refraction n,

$$n = n' - i\,n'', \tag{1.3}$$

we have for the electric field,

$$E_x = E_0 \exp[-2\pi\nu n''z]\, \exp[i2\pi\nu (ct - n'z)], \tag{1.4}$$

for the magnetic field,

$$H_y = n\, E_0 \exp[-2\pi\nu n''z]\, \exp[i2\pi\nu (ct - n'z)], \tag{1.5}$$

and for the real part of the cycle-averaged Poynting vector, $\langle N \rangle$, describing the spatial distribution of the energy density,

$$\langle N_z \rangle = \frac{1}{2}\left(\frac{c}{4\pi}\right) n' E_0^2 \exp[-4\pi\nu n'']. \tag{1.6}$$

As established in Appendix A, this leads to relationships between the susceptibility and the index of refraction

$$4\pi\chi' = n'^2 - 1 - n''^2, \tag{1.7}$$

$$4\pi\chi'' = 2\, n'\, n'', \tag{1.8}$$

and to the definition of the absorption coefficient per unit length (1/cm), κ ,

$$\kappa = 4\pi\nu n''. \tag{1.9}$$

For gases, Eqs. (1.7), and (1.8) are often expressed as

$$4\pi\chi' = 2(n' - 1), \tag{1.7a}$$

and

$$4\pi\chi'' = 2n'', \tag{1.8a}$$

where n' has been taken as $\simeq 1$, and $(n'^2 - 1) \gg n''^2$. Therefore, the absorption coefficient for gases is given in terms of the susceptibility by

$$\kappa = 8\pi^2 \nu \chi''. \tag{1.10}$$

The expression for the imaginary part of the susceptibility in terms of the power spectral density function $\phi(\nu)$ may be developed in three forms,

$$\chi''(\nu) = \frac{(1-e^{-\beta\nu})}{(1+e^{-\beta\nu})} [\phi(\nu) + \phi(-\nu)], \tag{1.11a}$$

$$\chi''(\nu) = (1-e^{-\beta\nu})\, \phi(\nu), \tag{1.11b}$$

and

$$\chi''(\nu) = \phi(\nu) - \phi(-\nu), \tag{1.11c}$$

where $\beta = hc/kT$. These three forms for $\chi''(\nu)$ are equivalent if $\phi(\nu)$ satisfies an important theorem, the fluctuation dissipation theorem (detailed balance)[5,6] which is given by

$$\phi(-\nu) = e^{-\beta\nu} \phi(\nu). \tag{1.12}$$

---

5. Kubo, R. The fluctuation-dissipation theorem, in Reports on Progress in Physics, Vol. XXIX Part 1, (1966), A.C. Stickland, Ed., The Institute of Physics and the Physical Society, London, pp 255-284.

6. Callen, H.B., and Welton, T.A. (1951) Irreversibility and generalized noise, Phys. Rev. 83:34-40.

If $\phi(\nu)$ does not satisfy detailed balance, then the form given by Eq. (1.11a) has certain attractive properties: radiation balance between emission and absorption is maintained independent of the correctness of $\phi(\nu)$, and $[\phi(\nu) + \phi(-\nu)]$ is an even function of ν and satisfies important summation properties.[1,7] It will prove convenient to write Eq. (1.11a) in the form

$$\chi''(\nu) = \tanh(\beta\nu/2)\ [\phi(\nu) + \phi(-\nu)], \tag{1.13}$$

We now assume that the imaginary part of the susceptibility may be obtained from the superposition of spectral contributions from individual transitions,

$$\chi''(\nu) = \sum_i \chi''_i(\nu) = \tanh(\beta\nu/2)\ \ \Sigma_i[\phi_i(\nu) + \phi_i(-\nu)], \tag{1.14}$$

where $\phi_i(-\nu) = e^{-\beta\nu}\phi_i(\nu)$.

At this stage, we make the impact approximation, obtaining

$$\chi''(\nu) = \tanh(\beta\nu/2)\ \ \sum_i S_i(m_p,T)[f_i(\nu, m_p,T) + f_i(-\nu,m_p,T)], \tag{1.15}$$

where for radiator density m_r (molec/cm^3), perturber density m_p (molec/cm^3), $S_i(m_r,T)$ (cm^{-1}) is the intensity associated with the i-th transition and $f_i(\nu,m_p,T)$ is the Lorentz function. The intensity S_i in terms of the transition strength μ_i^2 (debye^2) is given by

$$S_i(m_r,T) = m_r\ \frac{\pi}{3hc}\ 10^{-36}\ \mu_i^2\ [\rho_i''(T) + \rho_i'(T)], \tag{1.16}$$

for which ρ_i'' and ρ_i' are the fractional populations of the lower and upper states for the transition, respectively. The Lorentz function is defined through the expression

$$f_i(\nu,m_p,T) = \left(\frac{1}{\pi}\right) \frac{a_i(m_p,T)}{(\nu - \nu_i)^2 + a_i^2(m_p,T)}\ , \tag{1.17}$$

in which ν_i is the transition wavenumber value and $a_i(m_p,T)$ is the halfwidth. In collisional broadening of gases, the halfwidth is a linear function of perturber density expressed through the relationship

---

7. Van Vleck, J.H., and Huber, D.L. (1977) Absorption, emission, and linebreadths: a semihistorical perspective, Rev. Mod. Phys. 49, No. 4:939-959.

$$\alpha_i(m_p,T) = \left(\frac{m_p}{m_o}\right) \alpha_i^o(T). \tag{1.18}$$

The integral property of the function $f_i(\nu,m_p,T)$,

$$\int_{-\infty}^{\infty} f_i(\nu,m_p,T)\, d\nu = 1, \tag{1.19}$$

preserves the summation property of $[\phi(\nu) + \phi(-\nu)]$. In the impact approximation, the equivalency of Eqs. (1.11a) through (1.11c) is not preserved since

$$f(-\nu) \neq e^{-\beta\nu} f(\nu). \tag{1.20}$$

For clarity of presentation, the explicit dependence of $S_i(m_r,T)$, $f_i(\nu_i,m_p,T)$, and $\alpha_i(m_p,T)$ on m_r,m_p and T is suppressed, giving for the imaginary part of the susceptibility

$$\chi''(\nu) = \tanh(\beta\nu/2) \sum_i S_i [f_i(\nu) + f_i(-\nu)]. \tag{1.21}$$

It may readily be established that Eq. (1.21) reduces to the Van Vleck-Weisskopf[8] result for $\beta\nu \ll 1$ and to the infrared result for $\beta\nu \gg 1$.

Line coupling has become of increased interest because of its effects on spectral properties directly related to the remote sensing problem; the 60 GHz band for oxygen and the $\upsilon 67$ (cm^{-1}) Q branch for carbon dioxide. In this report, we will include the effects of a first order treatment of line coupling that also satisfies the condition of superposition. We have for the line coupling case in the impact approximation

$$\chi''(\nu) = \tanh(\beta\nu/2) \sum_i S_i [f_i(\nu) + y_i g_i(\nu) + f_i(-\nu) + y_i g_i(-\nu)], \tag{1.22}$$

where the line coupling coefficient y_i is linearly dependent on pressure and the function $g_i(\nu)$ is defined as

$$g_i(\nu) = \left(\frac{1}{\pi}\right) \frac{(\nu - \nu_i)}{(\nu - \nu_i)^2 + \alpha_i^2}. \tag{1.23}$$

---

8. Van Vleck, J.H., and Weisskopf, V.F. (1945) On the shape of collision-broadened lines, Rev. Mod. Phys. 17, Nos. 2 and 3:227-236.

We will consider the real part of the susceptibility in the impact approximation given by Eq. (1.21), for two limiting spectral domains, the millimeter and infrared regions, for which analytical results are available. A proposed analytical approximating function, consistent with the results in these two limiting spectral regions, is then developed for the real part of the susceptibility. We also develop an expression for the real part of the susceptibility by taking the Hilbert transform of Eq. (1.21) in which the tanh function is represented as a series expansion in terms of Lorentz functions. This result is then evaluated numerically to establish the validity of the proposed approximate function over the entire spectral domain.

Since the impact approximation does not provide an appropriate description for the line wing, as evidenced by its failure to satisfy detailed balance and to decay exponentially in the wing, we will discuss in Section 5 the effect of the wing contribution to the real part of the susceptibility.

2. THE KRAMERS-KRONIG RELATIONSHIP AND THE HILBERT TRANSFORM

The Kramers-Kronig relationship[9-16] plays the central role in our development by relating the real part, $\chi'(\nu)$, and the imaginary part, $\chi''(\nu)$, of the complex susceptibility, $\chi(\nu)$, through the Hilbert transform as

$$\chi'(\nu) = H[\chi''(\nu)] = (1/\pi) \int_{-\infty}^{\infty} \left[\frac{1}{(u - \nu)}\right] \chi''(u)\, du, \qquad (2.1a)$$

9. Bolton, H.C. (1969) Some practical properties of Kronig-Kramers transforms, The Philosophical Magazine, 19, No. 159:487-499.

10. Fahrenfort, J. (1963) The methods and results of dispersion studies, Chapter XI in Infra-red Spectroscopy and Molecular Structure, M.M. Davies Ed., Elsevier, New York, NY.

11. Huber, D.L., and Van Vleck, J.H. (1966) The role of Boltzmann factors in line shape, Rev. Mod. Phys. 38, No. 1:187-204.

12. Kramers, H.A. (1929) Die dispersion und absorption von Roentgenstrahlen, Physikalishe Zeitschrift, 30:522-523.

13. Kronig, R. de L, and Kramers, H.A. (1928) Absorption and dispersion in X-ray spectra, Z. Physik, 48, No. 3-4:174-179.

14. Kronig, R. de L. (1926) On the theory of dispersion of X-rays, J. Opt. Soc. Am. 12, No. 6:547-557.

15. Martin, P.C. (1967) Sum rules, Kramers-Kronig relations, and transport coefficients in charged systems, Phys. Rev., 161, No. 1:161-155.

16. Toll, J.S. (1956) Causality and the dispersion relation: logical foundations, Phys. Rev. 104, No. 6:1760-1770.

and the inverse transform as

$$\chi''(\nu) = H^{-1}[\chi'(\nu)] = -(1/\pi) \int_{-\infty}^{\infty} \left[\frac{1}{(u - \nu)}\right] \chi'(u)\, du. \qquad (2.1b)$$

It is noted that the Hilbert transform is unique up to an additive constant and, therefore, is defined for functions that vanish at infinity.

This relationship has been expressed in several alternative forms[17] including those described below:

$$\chi'(\nu) = (2/\pi) \int_{0}^{\infty} \left[\frac{1}{(u^2 - \nu^2)}\right] u\, \chi''(u)\, du, \qquad (2.2a, \text{Ref. } 10)$$

$$\chi''(\nu) = -(2/\pi) \int_{0}^{\infty} \left[\frac{1}{(u^2 - \nu^2)}\right] \nu\, \chi'(u)\, du, \qquad (2.2b, \text{Ref. } 5)$$

or

$$\chi'(\nu) = (2/\pi) \int_{0}^{\infty} \left[\frac{1}{(u^2 - \nu^2)}\right] [u\chi''(u) - \nu\chi''(\nu)]\, du, \qquad (2.3a, \text{Ref. } 15)$$

$$\chi''(\nu) = -(2/\pi) \int_{0}^{\infty} \left[\frac{1}{(u^2 - \nu^2)}\right] [\chi'(u) - \chi'(\nu)]\, du, \qquad (2.3b, \text{Ref. } 17)$$

The equivalence of Eqs. (2.1) and (2.2) can be shown by breaking the integral in Eq. (2.1) into two parts for the negative and positive range of the argument u and recombining them using the oddness of $\chi''(\nu)$, or the evenness of $\chi'(\nu)$. On the other hand, Eqs. (2.2) and (2.3) are equivalent since the principal value of

$$P \int_{0}^{\infty} \frac{Q}{(u^2 - \nu^2)}\, du = 0, \qquad (2.4)$$

for any constant Q.

---

17. Townes, C.H., and Schwalow, A.L. (1955) Microwave Spectroscopy, McGraw-Hill Book Company, New York, NY.

The relationship of the real and imaginary parts of the susceptibility can also be discussed in terms of the Fourier transform. Let $Y(t)$ be the inverse Fourier transform of the complex susceptibility $\chi(f)$, i.e., $Y(t) = \mathcal{F}^{-1}[\chi(f)]$. Note that for consistency with the conventional definition of the Fourier transform, $\chi(.)$ is a function of $f = \nu$ c with the frequency f in Hertz, whereas the Fourier transform pair is defined in terms of time t (sec) and frequency f (Hz) as below.

$$G(f) = \mathcal{F}[g(t)] = \int_{-\infty}^{\infty} g(t) e^{-i2\pi ft}\, dt, \tag{2.5a}$$

$$g(t) = \mathcal{F}^{-1}[G(f)] = \int_{-\infty}^{\infty} G(f) e^{+i2\pi ft}\, df. \tag{2.5b}$$

Now, $Y(t)$ is clearly a real and causal function because it represents a causal process of the wave-medium interaction. Therefore, its Fourier cosine and sine transforms can be associated with $\chi'(\nu)$ and $\chi''(\nu)$ respectively as follows:

$$\begin{aligned} \chi(f) &= \mathcal{F}[Y(t)] = \int_{-\infty}^{\infty} e^{-i2\pi ft}\, Y(t)\, dt, \\ &= \int_{0}^{\infty} (\cos 2\pi ft - i \sin 2\pi ft)\, Y(t)\, dt, \\ \chi(f) &= (1/2)\, \mathcal{F}_c[Y(t)] - i\,(1/2)\, \mathcal{F}_s[Y(t)], \\ &= \chi'(\nu) - i\, \chi''(\nu), \end{aligned} \tag{2.6}$$

where $\mathcal{F}_c[.]$ and $\mathcal{F}_s[.]$ denote the Fourier cosine and sine transforms defined as

$$\begin{aligned} G_c(f) &= \mathcal{F}_c[g(t)] = 2 \int_{0}^{\infty} \cos 2\pi ft\, g(t)\, dt, \\ g(t) &= \mathcal{F}_c^{-1}[G(f)] = 2 \int_{0}^{\infty} \cos 2\pi ft\, G_c(f)\, df, \end{aligned} \tag{2.7}$$

and

$$\begin{aligned} G_s(f) &= \mathcal{F}_s[g(t)] = 2 \int_{0}^{\infty} \sin 2\pi ft\, g(t)\, dt, \\ g(t) &= \mathcal{F}_s^{-1}[G(f)] = 2 \int_{0}^{\infty} \sin 2\pi ft\, G_s(f)\, df. \end{aligned} \tag{2.8}$$

Since for the causal function $Y(t)$, $Y(t) = 0$ for $t < 0$.

Hence we have

$$\chi'(f) = (1/2)\ \mathcal{F}_c[Y(t)],$$
$$\chi''(f) = (1/2)\ \mathcal{F}_s[Y(t)]. \tag{2.9}$$

Note that the change of variable is also needed here. After some algebra, the following alternate relationship can be obtained.

$$\chi'(f) = (1/4)\ \mathcal{F}_c[\ \mathcal{F}_s^{-1}[\ \chi''(\nu)]], \tag{2.10}$$

or, in an equivalent form

$$\chi'(f) = \int_0^\infty \cos 2\pi\ ft\ \left[\int_0^\infty \sin 2\pi\ ut\ \ \chi''(u)\ du\right] dt. \tag{2.11}$$

It is noted that all the real and imaginary parts appearing in these expressions have the required symmetry properties; the real parts are even functions and the imaginary parts are odd functions.

3. IMPACT LINE SHAPE

We consider the single transition susceptibility in this section for the sake of notational simplicity. In Eqs. (1.21) and (1.17), we eliminate the summation, utilize ν_0 in place of ν_i, and drop all other i subscripts. These may be reinvoked as the need arises.

The imaginary part of the complex susceptibility at wavenumber value ν due to a transition at ν_0 with intensity S (cm^{-1}) and half-width α(cm^{-1}) can be expressed as[11]

$$\chi''(\nu) = \tanh(\beta\nu/2)\ S\ [f(\nu) + f(-\nu)], \tag{3.1}$$

where $f(\nu)$ is the Lorentz line shape function as before,

$$f(\nu) = \frac{1}{\pi}\ \frac{\alpha}{(\nu - \nu_0)^2 + \alpha^2}. \tag{3.2}$$

It is useful to define a related function $g(\nu)$ where

$$g(\nu) = \frac{1}{\pi} \frac{(\nu - \nu_0)}{(\nu - \nu_0)^2 + \alpha^2} , \tag{3.3}$$

and to establish the following identities involving $f(\nu)$ and $g(\nu)$ that will be convenient for this study.

$$\nu f(\nu) = \nu_0 f(\nu) + \alpha g(\nu), \tag{3.4a}$$

$$\nu g(\nu) = -\alpha f(\nu) + \nu_0 g(\nu) + 1/\pi, \tag{3.4b}$$

$$\nu f(\nu) = -\nu_0 f(-\nu) - \alpha g(-\nu), \tag{3.4c}$$

$$\nu g(-\nu) = \alpha f(-\nu) - \nu_0 g(-\nu) - 1/\pi. \tag{3.4d}$$

These can be shown straightforwardly.

First we consider the millimeter wave region for which the impact result for $\chi(\nu)$ is well known.[8] For this spectral region, with $\beta\nu \ll 1$, we take

$$\tanh(\beta\nu/2) \simeq \beta\nu/2, \tag{3.5}$$

giving for the imaginary part,

$$\chi''(\nu)_{mm} = (\beta\nu/2)S\,[f(\nu) + f(-\nu)]. \tag{3.6}$$

Then the corresponding real part $\chi'(\nu)_{mm}$ is given by

$$\chi'(\nu)_{mm} = H[\chi''(\nu)_{mm}] = (S\beta/2)H[\nu f(\nu) + \nu f(-\nu)]$$

$$= (S\beta/2)H\Big[[\nu_0 f(\nu) + \alpha g(\nu)] - [\nu_0 f(-\nu) + \alpha g(-\nu)]\Big]. \tag{3.7}$$

The Hilbert transforms appearing in this equation are slight modifications of standard ones,[18] but are derived in the appendix because of their significance to our development. Using these results, we arrive at the final result for the millimeter region.

---

18. Bateman Manuscript Project, (1954) Tables of Integral Transforms, Vols. 1 and 2, McGraw-Hill, New York, NY.

$$\chi'(\nu):_{mm} = (S\beta\nu_0/2)\left[\left[(\alpha/\nu_0)f(\nu) - g(\nu)\right] + \left[(\alpha/\nu_0)f(-\nu) - g(-\nu)\right]\right]. \tag{3.8}$$

In the infrared case, for which $\beta\nu/2 \gg 1$, $\tanh(\beta\nu/2)$ may be approximated by unity. Since the Hilbert transform is defined over the entire real line and since it is essential to keep the symmetry property of tanh(.), we utilize the approximation

$$\tanh(\beta\nu/2) \approx \mathrm{sgn}(\nu), \tag{3.9}$$

where the signum function $\mathrm{sgn}(\nu)$ takes the value 1(-1) if the argument ν is positive (negative). Then $\chi''(\nu)$ can be approximated by

$$\chi''(\nu):_{IR} = S\ \mathrm{sgn}(\nu)\left[f(\nu) + f(-\nu)\right]. \tag{3.10}$$

Then the corresponding real part of the susceptibility is

$$\chi'(\nu):_{IR} = H[\chi''(\nu):_{IR}] = (1/\pi)\int_{-\infty}^{\infty} \chi''(u):_{IR} / (u-\nu)\, du. \tag{3.11}$$

Evaluating the principal value of the integrals in this equation, we obtain,

$$\chi'(\nu):_{IR} = -(2S/\pi)\tan^{-1}(\nu_0/\alpha)\left[g(\nu) + g(-\nu)\right] + (S/\pi)\ln\left[\frac{\nu_0^2+\alpha^2}{\nu^2}\right]\left[f(\nu) + f(-\nu)\right]. \tag{3.12}$$

Using the infrared approximation $\nu_0/\alpha \gg 1$, and assuming $\nu = \nu_0$, this equation may be simplified to

$$\chi'(\nu):_{IR} = -S\left[g(\nu) + g(-\nu)\right]. \tag{3.13}$$

The elimination of the logarithm and the setting of the $\tan^{-1}$ function at $\pi/2$ may be viewed as eliminating the spurious discontinuity of Eq. (3.10) at the origin ($\nu = 0$). The discontinuity is spurious since it arises from approximating $\tanh(\beta\nu/2)$ by $\mathrm{sgn}(\nu)$ and this approximation is not valid in the vicinity of the origin.

The result given by Eq. (3.13) for $\chi'(\nu):_{IR}$ may be obtained directly by approximating $\chi''(\nu)$ in Eq. (3.11),

$$\chi''(\nu):_{IR2} = S\left[f(\nu) - f(-\nu)\right]. \tag{3.14}$$

It is illuminating to note that this form of $\chi''(\nu)$ is consistent with the form given by one of the alternate expressions for the imaginary part of the susceptibility in terms of the power spectral density function, Eq. (1.4c). This approximate form for $\chi''(\nu)$ has an advantage over that given in Eq. (3.10) since it has no discontinuity at the origin, and consequently will prove to be useful when we consider the line coupling problem in Section 4.

To study the transition of $\chi'(\nu)$ from one spectral regime to the other, we first consider the delta line shape function. With the delta line shape function, the exact Hilbert transform can be obtained without using approximations to the $\tanh(\beta\nu/2)$ function. Thus by replacing $f(\nu)$ in Eq. (3.1) by the delta function $\delta(\nu - \nu_0)$, we obtain

$$\chi'(\nu) = H\left[\tanh(\beta\nu/2)\, S\,[\delta(\nu - \nu_0) + \delta(\nu + \nu_0)]\right]$$

$$= S\tanh(\beta\nu_0/2)\left[\frac{1}{(\nu_0 - \nu)} + \frac{1}{(\nu_0 + \nu)}\right]$$

$$= 2S\tanh(\beta\nu_0/2)\left[\frac{\nu_0}{\nu_0^2 - \nu^2}\right]. \qquad (3.15)$$

This expression suggests that if the line shape function, $f(\nu)$, is narrow compared to the variation of the $\tanh(\beta\nu/2)$ function, then the transition of the magnitude of $\chi'(\nu)$ from the millimeter to the infrared is specified by the same $\tanh(\beta\nu/2)$ function as for $\chi''(\nu)$ except that $\tanh(\beta\nu/2)$ is evaluated at the line center $\nu = \nu_0$.

Considering the two results in Eqs. (3.8 and (3.13), and the above observation, we now postulate the following real part of the susceptibility for use in both millimeter and infrared regions.

$$\chi'_p(\nu) = S\tanh(\beta\nu_0/2)\left[[-g(\nu) + (\alpha/\nu_0)f(\nu)]\right.$$

$$\left. + [-g(-\nu) + (\alpha/\nu_0)f(-\nu)]\right]. \qquad (3.16)$$

This result reduces to the millimeter result in Eq. (3.8) by letting $\beta\nu_0/2$ become small, and to the infrared result in Eq. (3.13) by letting $\beta\nu_0/2$ become large and α/ν_0 small.

We now perform the inverse Hilbert transform of $\chi'_p(\nu)$ to obtain $\chi''_p(\nu)$ for comparisons with previously used expressions,

$$\chi''_p(\nu) = H^{-1}[\chi'_p(\nu)] = -H[\chi'_p(\nu)]$$

$$= S(\nu/\nu_0)\tanh(\beta\nu_0/2)\left[f(\nu) + f(-\nu)\right]. \qquad (3.17)$$

For the millimeter case, the approximation $\tanh(\beta\nu/2) \simeq \beta\nu/2$ reduces this result to Eq. (3.6). On the other hand, for the infrared case, $\tanh(\beta\nu_0/2) \simeq 1$, Eq. (3.17) gives

$$\chi''_p(\nu)_{IR} = S(\nu/\nu_0)\left[f(\nu) + f(-\nu)\right] . \tag{3.18}$$

The expression states that the proposed real part gives rise to a linear approximation ν/ν_0 for the $\tanh(\beta\nu/2)$ function in the infrared region. It is essential to note that this function is a valid approximation in the infrared for frequencies near the line center for which ν is large and $\nu \simeq \nu_0$.

The $\tanh(\beta\nu_0/2)$ dependence in Eq. (3.16) suggests that the proposed real part might be obtained through the line center approximation defined by the replacement of $\tanh(\beta\nu/2)$ by $\tanh(\beta\nu_0/2)$ and then taking the Hilbert transform. However, the existence of the second and the fourth terms in $\chi'_p(\nu)$ proves otherwise. It will be shown later, however, that the major contribution to the Hilbert transform comes from the line center rather than the line wing. This gives a rationalization for the $\tanh(\beta\nu_0/2)$ dependence of the proposed real part.

4. IMPACT LINE SHAPE WITH LINE COUPLING

Although the inclusion of line coupling in the determination of the imaginary part of the susceptibility for a molecular system is in general a complex problem, a first order treatment has been developed in which superposition is preserved.[19-21] In our formalism, the imaginary part of the susceptibility may be expressed as,

$$\chi''_c(\nu) = \sum_i S_i \tanh(\beta\nu/2)\left[f_i(\nu) + y_i g_i(\nu) + f_i(-\nu) + y_i g_i(-\nu)\right] , \tag{4.1}$$

where y_i is the line coupling coefficient, which in general will be subject to the constraint[21],

$$\sum_i S_i y_i = 0 , \tag{4.2}$$

---

19. Baranger, M. (1958) Problem of overlapping lines in the theory of pressure broadening, Phys. Rev. 111, No. 2:494-504.

20. Rosenkranz, P.W. (1975) Shape of the 5 mm oxygen band in the atmosphere, IEEE Trans. Ant. Propagat., AP-23, No. 4:498-505.

21. Smith, E.W. (1981) Absorption and dispersion in the O_2 microwave spectrum at atmospheric pressures, J. Chem. Phys., 74:6658-6673.

referred to as the zero-sum rule. The spectral properties of $\chi''(\nu)$ for overlapped lines are dependent on this zero-sum rule, and the relationship of the γ_i to the a_i.

At this stage in the development, we drop the summation from Eq. (4.1) and adopting the notation of Section 3, we obtain the imaginary part of the susceptibility associated with a single transition,

$$\chi''_c(\nu) = S \tanh(\beta\nu/2) \left[f(\nu) + yg(\nu) + f(-\nu) + yg(-\nu) \right] . \tag{4.3}$$

We again start in the millimeter spectral regime, where $\tanh(\beta\nu/2) \simeq \beta\nu/2$, for which we obtain,

$$\chi''_c(\nu)_{:mm} = S\,(\beta\nu/2) \left[f(\nu) + yg(\nu) + f(-\nu) + yg(-\nu) \right] . \tag{4.4}$$

Using the previously established identities among $f(\nu)$ and $g(\nu)$ given in Eq. (3.4), we obtain

$$\chi''_c(\nu)_{:mm} = (S\beta/2) \left[\left[(\nu_0 + ya)f(\nu) + (a + y\nu_0)g(\nu) \right] + y/\pi \right.$$
$$\left. - \left[(\nu_0 - ya)f(-\nu) + (a + y\nu_0)g(-\nu) \right] - y/\pi \right] \tag{4.5}$$

We may cancel $\pm y/\pi$ terms in this expression and obtain,

$$\chi''_c(\nu)_{:mm} = (S\beta/2) \left[\left[(\nu_0 - ya)f(\nu) + (a + y\nu_0)g(\nu) \right] \right.$$
$$\left. - \left[(\nu_0 - ya)f(-\nu) + (a + y\nu_0)g(-\nu) \right] \right] . \tag{4.6}$$

We now take the Hilbert transform of Eq. (4.6) to obtain the real part of the susceptibility for the line coupled case in the millimeter region, obtaining

$$\chi'_c(\nu)_{:mm} = H[\chi''_c(\nu)_{:mm}]$$
$$= (S\beta/2) \left[\left[-(\nu_0 - ya)g(\nu) + (a + y\nu_0)f(\nu) \right] \right.$$
$$\left. + \left[-(\nu_0 - ya)g(-\nu) + (a + y\nu_0)f(-\nu) \right] \right] . \tag{4.7a}$$

$$\chi'_c(\nu)_{:mm} = (S\beta\nu_0/2) \left[\left[-(1 - ya/\nu_0)g(\nu) + (a/\nu_0 + y)f(\nu) \right] \right.$$
$$\left. + \left[-(1 - ya/\nu_0)g(-\nu) + (a/\nu_0 + y)f(-\nu) \right] \right] . \tag{4.7b}$$

Thus, the significance of Eq. (4.6) for $\chi''_c(\nu)$ is that its Hilbert transform is well defined and the inverse Hilbert transform of the corresponding $\chi'_c(\nu)$ matches the original expression. Thus the difficulty encountered in taking the Hilbert transform of Eq. (4.4) in earlier studies is eliminated.

It is straightforward to check the agreement of the inverse Hilbert transform of this expression with $\chi''_c(\nu)$ given in Eq. (4.6).

For the infrared region, in which $\tanh(\beta\nu/2) \simeq 1$, we use the form given by Eq. (3.14) for the line-coupled imaginary part,

$$\chi''_c(\nu):_{IR} = S\left[[f(\nu) + yg(\nu)] - [f(-\nu) + yg(-\nu)]\right] . \tag{4.8}$$

The corresponding real part $\chi'_c(\nu):_{IR} = H[\chi''_c(\nu):_{IR}]$ is then obtained as

$$\chi'_c(\nu):_{IR} = -S\left[[g(\nu) + yf(\nu)] + [g(-\nu) - yf(-\nu)]\right] . \tag{4.9}$$

The real part of the susceptibility without line coupling for the limiting spectral regions, given by Eqs. (3.8) and (3.13), can be obtained from these expressions including line coupling by setting $y = 0$.

As in the development for the case without line coupling, we examine expressions for two limiting spectral regions, Eqs. (4.7) and (4.9), and postulate the following form for the real part of the susceptibility with line coupling

$$\chi'_{cp}(\nu) = S\tanh(\beta\nu_0/2)\left[[-g(\nu) + (\alpha/\nu_0)f(\nu)] + y[f(\nu) + (\alpha/\nu_0)g(\nu)]\right.$$
$$\left. + [-g(-\nu) + (\alpha/\nu_0)f(-\nu)] + y[f(-\nu) + (\alpha/\nu_0)g(-\nu)]\right] . \tag{4.10a}$$

Two equivalent forms for this proposed function are given as

$$\chi'_{cp}(\nu) = S\tanh(\beta\nu_0/2)\,[-(1 - y\alpha/\nu_0)g(\nu) + (\alpha/\nu_0 + y)f(\nu)$$
$$- (1 - y\alpha/\nu_0)g(-\nu) + (\alpha/\nu_0 + y)f(-\nu)] , \tag{4.10b}$$

and

$$\chi'_{cp}(\nu) = (S/\pi)\tanh(\beta\nu_0/2)$$
$$\left[\frac{[-(\nu - \nu_0) + \alpha^2/\nu_0 + y\alpha\nu/\nu_0]}{[(\nu - \nu_0)^2 + \alpha^2]} + \frac{[(\nu + \nu_0) + \alpha^2/\nu_0 - y\alpha\nu/\nu_0]}{[(\nu + \nu_0)^2 + \alpha^2]}\right] . \tag{4.10c}$$

The agreement of the proposed function, Eq. (4.10), with expressions for the limiting spectral regions may readily be established by allowing $\beta \nu_0 \ll 1$ for the millimeter region and by taking $\beta \nu_0 \gg 1$, $\alpha / \nu_0 \simeq 0$ and $y \leq 1$ for the infrared region. We next examine the validity of this real part by taking the inverse Hilbert transform and comparing the result with the original imaginary part. Using Eq. (4.10b), we derive

$$\chi''_{cp}(\nu) = H^{-1}[\chi'_{cp}(\nu)] = -H[\chi'_{cp}(\nu)]$$

$$= S \tanh(\beta \nu_0/2) \left[[(1 - y\alpha/\nu_0)f(\nu) + (\alpha/\nu_0 + y)g(\nu)] \right.$$

$$\left. - [(1 - y\alpha/\nu_0)f(-\nu) + (\alpha/\nu_0 + y)g(-\nu)] \right] . \qquad (4.11)$$

The millimeter limit can easily be checked using the approximation, $\tanh(\beta \nu_0/2) \simeq \beta \nu_0/2$. On the other hand, the infrared approximation, $\tanh(\beta \nu_0/2) \simeq 1$, and $\alpha/\nu_0 \simeq 0$, once again gives the correct result. Thus the appropriateness of the proposed real part given by Eq. (4.10) has been demonstrated.

5. LINE WING CONTRIBUTIONS

The question arises as to whether the real part of the susceptibility, obtained through the Hilbert transform, depends critically on the line wing of the imaginary part. This issue is an important one because if it does, then the use of the impact line shape would be expected to introduce a significant error in the result for the real part. This is because the impact line shape is known to be inappropriate for the line wings.[22] This section is devoted to the consideration of this important point.

An intuitive approach would be to compare a line shape function having a substantially different form for the line wing with the impact result. While the use of the Gaussian function for $\chi''(\nu)$ would serve this purpose, the lack of a simple closed form expression for the Hilbert transform of the Gaussian suggests the desirability of an alternative approach. Let us consider a function for $\chi''(\nu)$ constructed as the difference of two Lorentzian functions having different strengths and widths. This approach has two advantages: the Hilbert transform is available and the difference function can be made to have an asymptotic behavior significantly different from that of a single Lorentz function.

---

22. Clough, S.A., Kneizys, F.X., Davies, R., Gamache, R., and Tipping, R. (1980) Theoretical line shape for H_2O vapor: application to the continuum, in Atmospheric Water Vapor, A. Deepak, T.D. Wilkerson, and L.H. Ruhnke, Eds., Academic Press, New York, NY, pp 25-46.

For clarity of the presentation, we consider the simple Lorentz function in the infrared region. Let $L(\nu)$ and $L_d(\nu)$ be the simple Lorentz and the modified Lorentz profiles centered at $\nu = \nu_0$ and be defined by

$$L(\nu) = f(\nu). \tag{5.1}$$

$$L_d(\nu) = m_1 f(\nu) - m_2 f_2(\nu), \tag{5.2}$$

where the Lorentz function $f(\nu)$ has a line width α, and $f_2(\nu)$ in Eq. (5.2) has a line width α_2. The integrated strengths of the two profiles, $L(\nu)$ and $L_d(\nu)$, are maintained through the relationship

$$m_1 - m_2 = 1. \tag{5.3}$$

Equation (5.2) may be rewritten as

$$L_d(\nu) = \frac{1}{\pi} \frac{[(m_1\alpha - m_2\alpha_2)(\nu - \nu_0)^2 + \alpha\alpha_2(m_1\alpha_2 - m_2\alpha)]}{[(\nu - \nu_0)^2 + \alpha^2]\,[(\nu - \nu_0)^2 + \alpha_2^2]}. \tag{5.4}$$

Setting

$$m_1\alpha = m_2\alpha_2, \tag{5.5}$$

the ν dependence of the numerator of Eq. (5.4) is eliminated. As a consequence, the new line function asymptotically approaches zero as ν^{-4} rather than ν^{-2} of the original function. Thus a simple modification has provided a significant difference in the asymptotic behavior of the line shape.

We define the ratio of the halfwidths of the two Lorentz functions in Eq. (5.2) to be r, namely, $r = \alpha/\alpha_2$. Then Eq. (5.5) can be written as

$$\frac{m_2}{m_1} = \frac{\alpha}{\alpha_2} = r. \tag{5.6}$$

Then Eqs. (5.3) and (5.6) can be combined to give

$$m_1 = \frac{1}{(1 - r)} \tag{5.7}$$

$$m_2 = \frac{r}{(1 - r)} \tag{5.8}$$

Because our intention is to alter the line wing without appreciably affecting the center, we assume the ratio r to be small.

Using these two line shape functions and the infrared approximation in Eq. (3.14), the real parts $\chi'(\nu)$ and $\chi'_d(\nu)$ can be obtained as

$$\chi'(\nu) = - S\, g(\nu), \text{ and} \tag{5.9}$$

$$\chi'_d(\nu) = - S \left[\frac{1}{1 - r}\, g(\nu) - \frac{r}{1 - r}\, g_2(\nu)\right]. \tag{5.10}$$

where $g(\nu)$ and $g_2(\nu)$ have halfwidths α and α_2 respectively. After some manipulation, Eq. (5.10) becomes

$$\chi'_d(\nu) = \chi'(\nu)\left[1 + r \left[1 - \frac{(\nu - \nu_0)^2 + r^2 \alpha_2^2}{(\nu - \nu_0)^2 + \alpha_2^2}\right]\right] . \tag{5.11}$$

Now we can compare this with the original impact result. Far from the line center, for which $: \nu - \nu_0 :>> \alpha_2$, the inner bracket vanishes and Eq. (5.11) reduces to

$$\chi'_d(\nu)_{:far} \sim \chi'(\nu)_{:far} . \tag{5.12}$$

Thus, the important result is obtained that the real part of the susceptibility far from the line center is relatively unaffected by the change in the asymptotic property of the imaginary part.

On the other hand, near the line center where $: \nu - \nu_0 :<< \alpha_2$, Eq. (5.11) leads to

$$\chi'_d(\nu)_{:near} \sim (1 + r)\ \chi'(\nu)_{:near} , \tag{5.13}$$

through the second order in r. This small change in magnitude may be associated with the change in the magnitude near the line center of the imaginary part, namely, for $: \nu - \nu_0 :<< \alpha_2$,

$$\chi''_d(\nu)_{:near} \sim (1 + r)\ \chi''(\nu)_{:near} , \tag{5.14}$$

through the first order in r. Comparison of Eq. (5.13) with Eq. (5.14) suggests that the slight change in the magnitude of the real part near the line center is attributable to the small change in the imaginary part near the line center.

To provide a sense of the magnitude of r, let us consider numerical values appropriate to the molecular collision broadening problem. We take α to be 0.1 cm^{-1} and if we assume α_2 to be 10 cm^{-1}, we obtain a value for r,

$$r = \frac{0.1}{10} = 0.01 \ . \tag{5.15}$$

It should be noted that for small values of r, the ratio of the magnitudes of the two real functions, $\chi''_d(\nu_0 \pm \alpha_2)/\chi''(\nu_0 \pm \alpha_2)$, is approximately one-half. Thus, when r = 0.01, the modified line profile is about one-half the value of the Lorentz profile 10 cm^{-1} away from the line center. The magnitude of the real part near the line center is increased by the factor 1.01 (Eq. (5.13)), and far from the line center, $|\nu - \nu_0| \gg 10\ cm^{-1}$, the real part is unaffected by the reduction of the line wing (Eq. (5.12)).

6. SERIES EXPRESSION FOR EXACT REAL PART

We now address the evaluation of the exact real part of the susceptibility. An exact expression for $\chi'(\nu)$ in an infinite series form is derived using a known expansion of the tanh(.) function using Lorentz functions is given by Gradshteyn.[23]

$$\tanh(\pi x/2) = (4x/\pi)\sum_{k=1}^{\infty} \frac{1}{x^2 + (2k-1)^2} \tag{6.1}$$

We substitute this in Eq. (4.1) to obtain

$$\chi''(\nu) = 4S/\beta \sum_{k=1}^{\infty} \frac{\nu}{\nu^2 + e(k)^2} \left[f(\nu) + \gamma g(\nu) + f(-\nu) + \gamma g(-\nu) \right] , \tag{6.2}$$

23. Gradshteyn, I.S. and Ryzhik, I.M. (1980) Table of Integrals, Series, and Products A. Jeffrey Trans., Academic Press, New York, NY.

where

$$e(k) = \frac{(2k - 1)\pi}{\beta}. \tag{6.3}$$

This result provides a series expansion of the impact line shape including line coupling. From this expression it is straight-forward to obtain the Hilbert transform of $\chi''(\nu)$. In fact, the partial fraction expansion of the summand gives

$$\chi''(\nu) = 4S/\beta \sum_{k=1}^{\infty} \left[\frac{2A(k)\nu}{\nu^2+e(k)^2} + [B(k)f(\nu) - A(k)g(\nu)] \right.$$

$$\left. - [B(k)f(-\nu) - A(k)g(-\nu)] \right] , \tag{6.4}$$

with

$$A(k) = \frac{\alpha(\nu_0^2+\alpha^2-e(k)^2) - y\nu_0(\nu_0^2+\alpha^2+e(k)^2)}{D(k)}, \tag{6.5a}$$

$$B(k) = \frac{\nu_0(\nu_0^2+\alpha^2+e(k)^2) + y\alpha(\nu_0^2+\alpha^2-e(k)^2)}{D(k)}, \tag{6.5b}$$

$$D(k) = (\nu_0^2+\alpha^2-e(k)^2)^2 + 4\nu_0^2 e(k)^2 . \tag{6.5c}$$

Because the series converges absolutely, the Hilbert transform and the summation can be interchanged. Thus the desired result is obtained,

$$\chi'(\nu) = H[\chi''(\nu)]$$

$$= (4S/\beta) \sum_{k=1}^{\infty} \left[\frac{2A(k)e(k)}{\nu^2 + e(k)^2} - [B(k)g(\nu) + A(k)f(\nu)] - [B(k)g(-\nu) \right.$$

$$\left. - [B(k)g(-\nu) + A(k)f(-\nu)] \right] . \tag{6.6}$$

This series expression will be used for the numerical verification of the accuracy of the proposed real part $\chi'_{cp}(\nu)$.

For ease of computation, we rewrite this equation in the form:

$$\chi'(\nu) = (4S/\beta) \sum_{k=1}^{\infty} \frac{2A(k)e(k)}{[\nu^2 + e(k)^2]}$$

$$- (4S/\beta)\,[f(\nu) + f(-\nu)] \sum_{k=1}^{\infty} A(k)$$

$$- (4S/\beta)\,[g(\nu) + g(-\nu)] \sum_{k=1}^{\infty} B(k)\ . \qquad (6.7)$$

Although the first summation has to be computed for each wavenumber value ν, the second and third summations need only be evaluated once for a given transition since they are independent of ν. It is noted that the convergence rates of the series are of the order of $1/k^3$ for the first summation and of $1/k^2$ for the other two summations. This expression provides a viable procedure for calculating $\chi'(\nu)$ from $\chi''(\nu)$ in the impact approximation for a limited number of transitions at a limited number of wavenumber values.

The exact real part of the susceptibility in Eq. (6.7) and the proposed function given by Eq. (4.10) have been compared numerically for three values of the line center, ν_0 = 10, 410, and 1500 cm^{-1}, which represent transitions located in the millimeter, intermediate, and infrared regions, respectively. The choice of ν_0 = 410 cm^{-1} has been made because it provides $\beta\nu_0/2 \simeq 1$ for room temperature, T = 296 (K), where neither the approximation for tanh(.) of Eq. (3.5) or of Eq. (3.9) is appropriate. Typical values of S = 2.0 cm^{-1} and α = 0.1 cm^{-1} have been used for computations throughout.

Two runs have been performed for each value of the line center: once for the line center region, ν_0 -1 cm^{-1} to ν_0 + 1 cm^{-1} at a sampling interval of 0.01 cm^{-1}, and the second for wide ranges spanning from 1 to 10^4 cm^{-1} for the millimeter case and from 10 to 10^5 cm^{-1} for other cases at appropriate sampling intervals.

The line coupling effects have been evaluated by considering doublets centered at wavenumber values $\nu_0 \pm \alpha$, providing a separation 2α = 0.2 cm^{-1}, and with the coupling coefficients $y_i = \pm 0.1$. The convergence criterion that the ratio of the new iteration term to the accumulated sum be less than a prechosen small number $\epsilon = 10^{-6}$ has been

utilized for terminating the first summation in Eq. (6.7), and the numbers of iterations needed for convergence have been recorded for each run. The two other summations, evaluated only once for each line, have been computed to a specified maximum number of iterations for which satisfactory convergence is assured. Additional trial runs were also performed for various convergence critera, $\epsilon = 10^{-3}$, 10^{-4}, and 10^{-5}, to assess the convergence property of the first summation of Eq. (6.7). The results showed 20, 40, and 80 iterations on the average to reach the convergence, in contrast to an average of 180 iterations for the runs with $\epsilon = 10^{-6}$. This indicates that the series expression obtained for the exact real part could be used in computational application, provided the number of transitions is small.

The results obtained are summarized in Figures 1 through 3 and Table 1. Figures 1-A through 1-C represent the line center computations for millimeter, intermediate, and infrared regions, respectively, for a single line. Each figure consists of three plots; the imaginary part $\chi''(\nu)$, the proposed real part $\chi'_p(\nu)$ of the susceptibility, and the difference between the proposed and the exact real parts $\chi'_p(\nu) - \chi'(\nu)$. Figures 2-A through 2-C indicate the difference over wider regions for the single line cases. Figures 3-A through 3-C represent computations for two lines with line coupling. Table 1 summarizes the error computations. It includes the number of terms required for the convergence of the first summation in the series expression, Eq. (6.7), for the exact real part of the susceptibility.

7. DISCUSSIONS AND CONCLUSIONS

A unified and analytic approximate real part of the susceptibility over the entire millimeter and infrared regions that is consistent with the Van Vleck-Huber impact line shape with line coupling has been proposed. Fundamental to our derivation is the assumption of superposition, namely that the complex susceptibility for the system may be obtained from the contributions to the susceptibility from the individual transitions. This assumption allows us to apply the Hilbert transform and its inverse to the real and imaginary parts for a single transition to establish the Kramers-Kronig relationship for the system. The proposed real part of the susceptibility has been obtained through careful examination of two limiting cases of the millimeter and infrared spectral regions for which the real parts have been explicitly computed from the respective limiting forms of the imaginary part. The inverse Hilbert transform of the proposed real part was computed to demonstrate consistency with the original function.

Although for the line coupling case, the zero-sum rule is an important element of the spectral property of both the real and imaginary parts of the susceptibility for the molecular system, its utilization has not been necessary in the development of the proposed function. An important requirement in our formulation, necessary to maintain

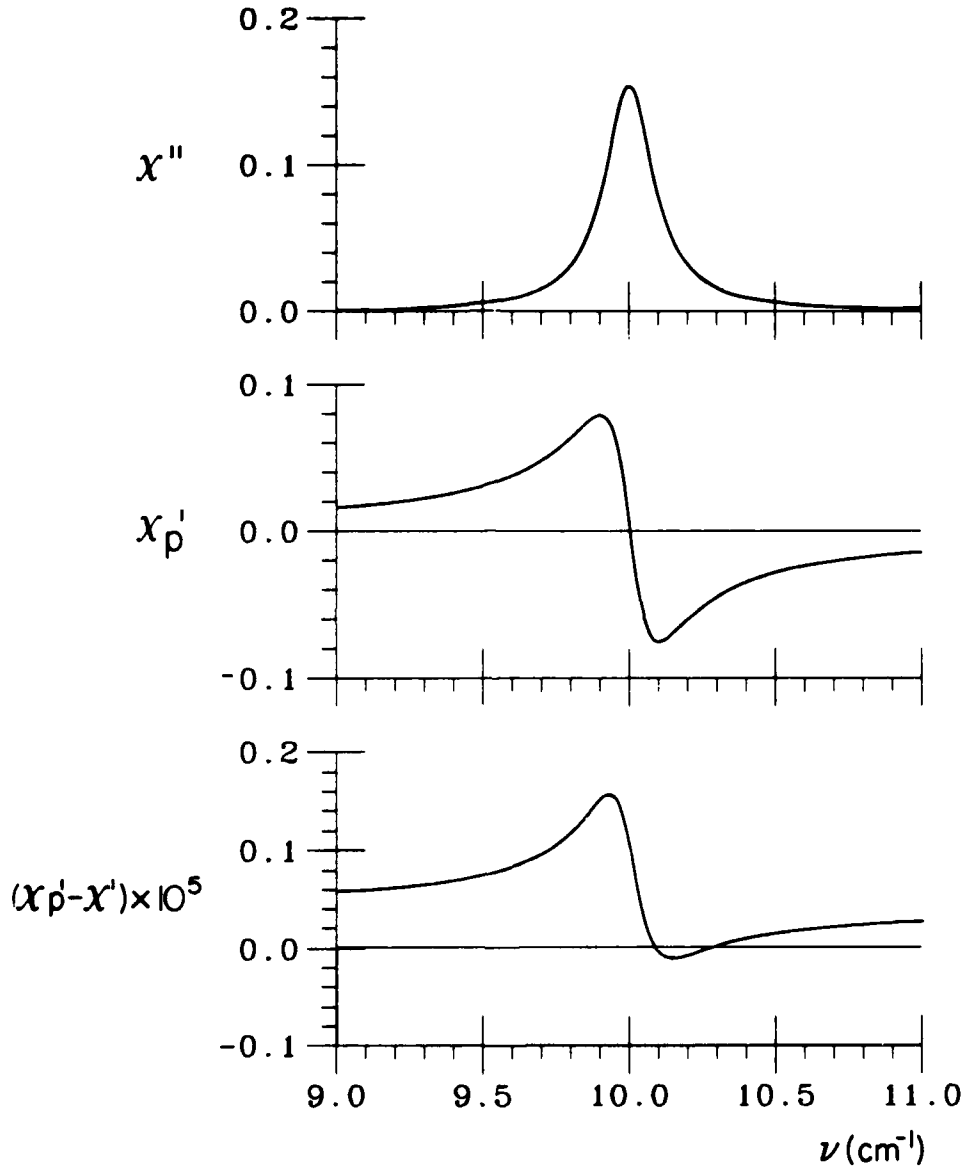

Figure 1A. Imaginary part of the susceptibility (χ''), proposed real part of the susceptibility (χ'_p), and the difference between the proposed and actual real part ($\chi'_p - \chi'$) as a function of wavenumber for a single line with strength of 2 cm^{-1} at 10 cm^{-1} and a halfwidth of 0.1 cm^{-1}

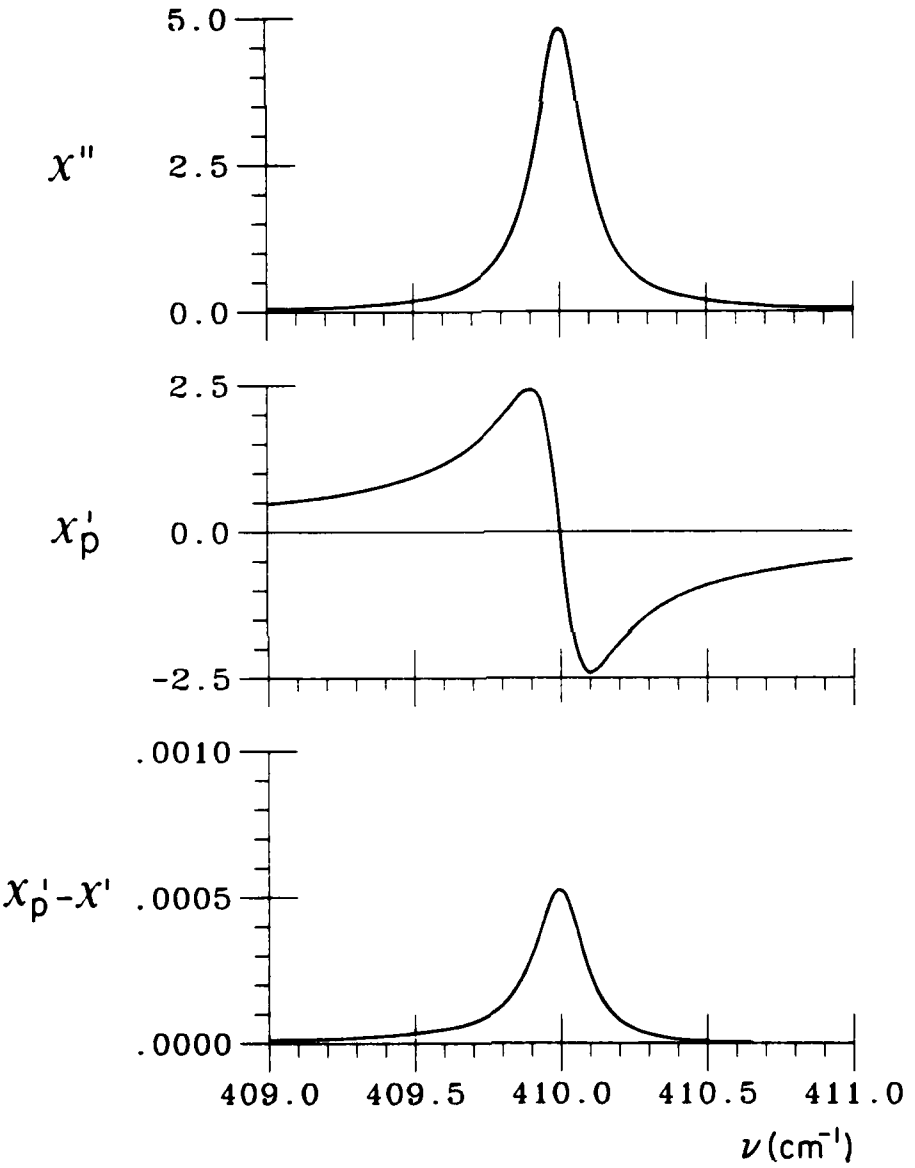

Figure 1B. Imaginary part of the susceptibility (χ''), proposed real part of the susceptibility (χ'_p), and the difference between the proposed and actual real part ($\chi'_p - \chi'$) as a function of wavenumber for a single line with strength of 2 cm^{-1} at 410 cm^{-1} and a halfwidth of 0.1 cm^{-1}

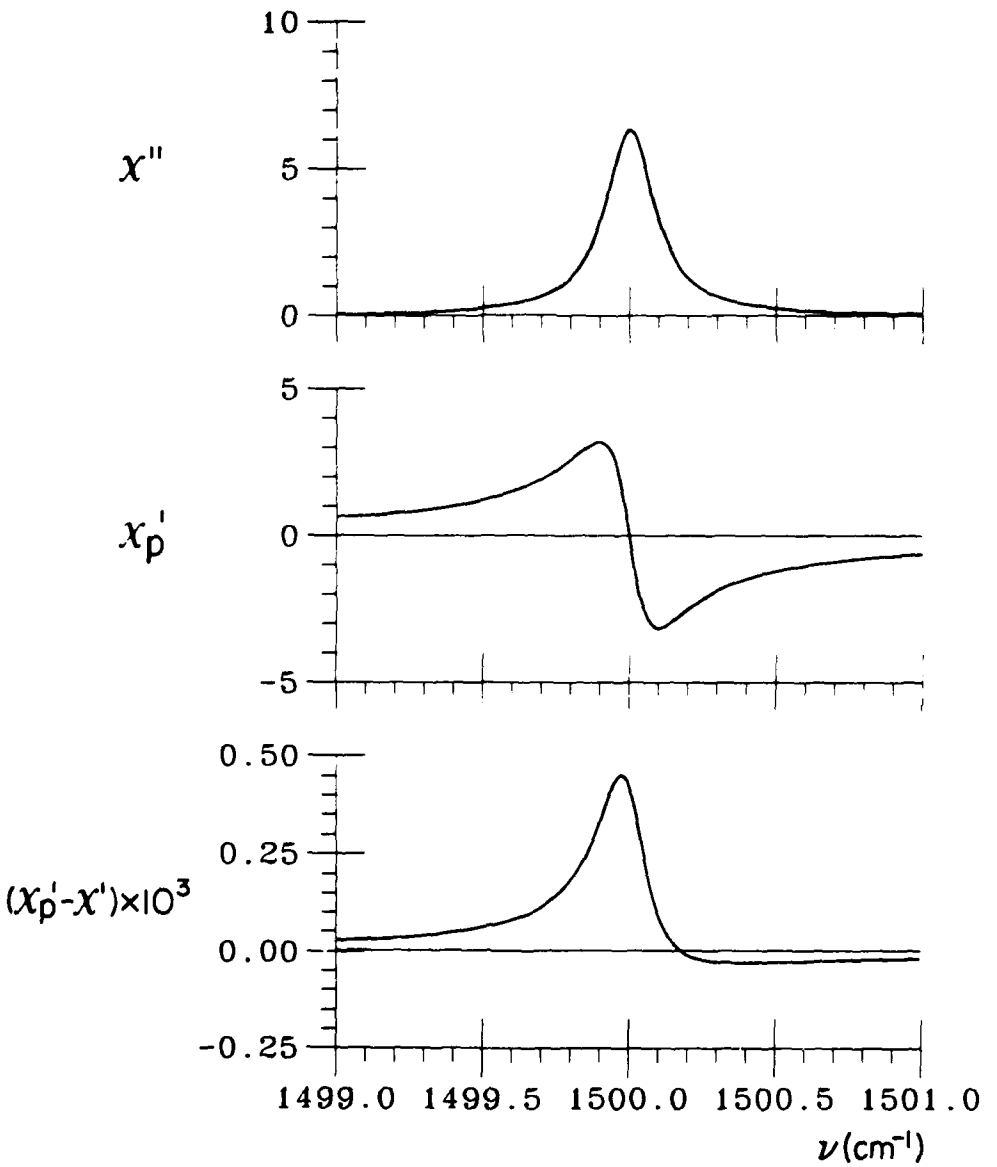

Figure 1C. Imaginary part of the susceptibility (χ "), proposed real part of the susceptibility (χ'_p), and the difference between the proposed and actual real part ($\chi'_p - \chi'$) as a function of wavenumber for a single line with strength of 2 cm^{-1} at 1500 cm^{-1} and a halfwidth of 0.1 cm^{-1}

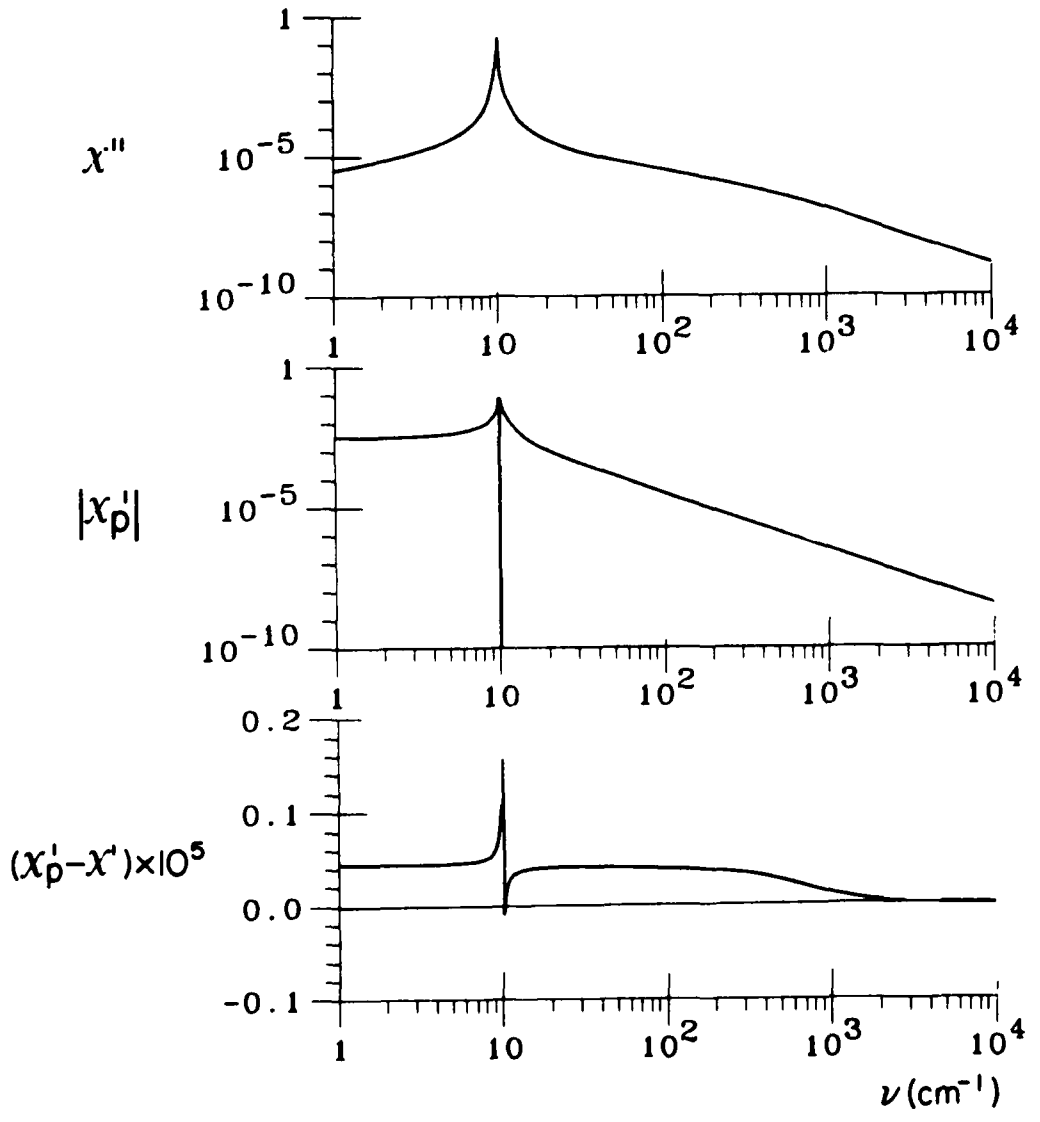

Figure 2A. Imaginary part of the susceptibility (χ''), magnitude of proposed real part of the susceptibility (χ'_p), and the difference between the proposed and actual real part ($\chi'_p - \chi'$) over an expanded spectral range for a single line with strength of 2 cm^{-1} at 10 cm^{-1} and a halfwidth of 0.1 cm^{-1}

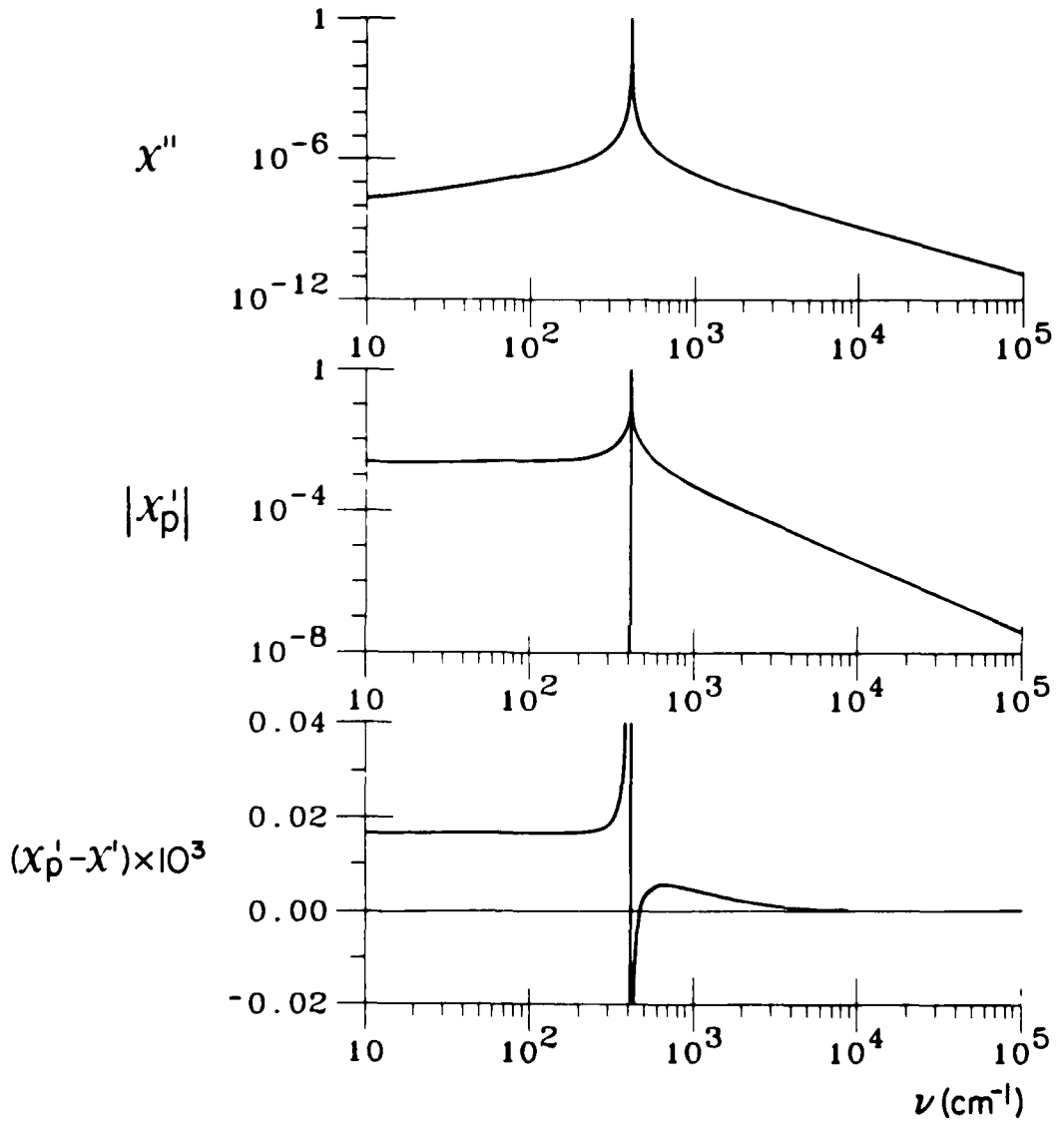

Figure 2B. Imaginary part of the susceptibility (χ''), magnitude of proposed real part of the susceptibility (χ'_p), and the difference between the proposed and actual real part ($\chi'_p - \chi'$) over an expanded spectral range for a single line with strength of 2 cm^{-1} at 410 cm^{-1} and a halfwidth of 0.1 cm^{-1}

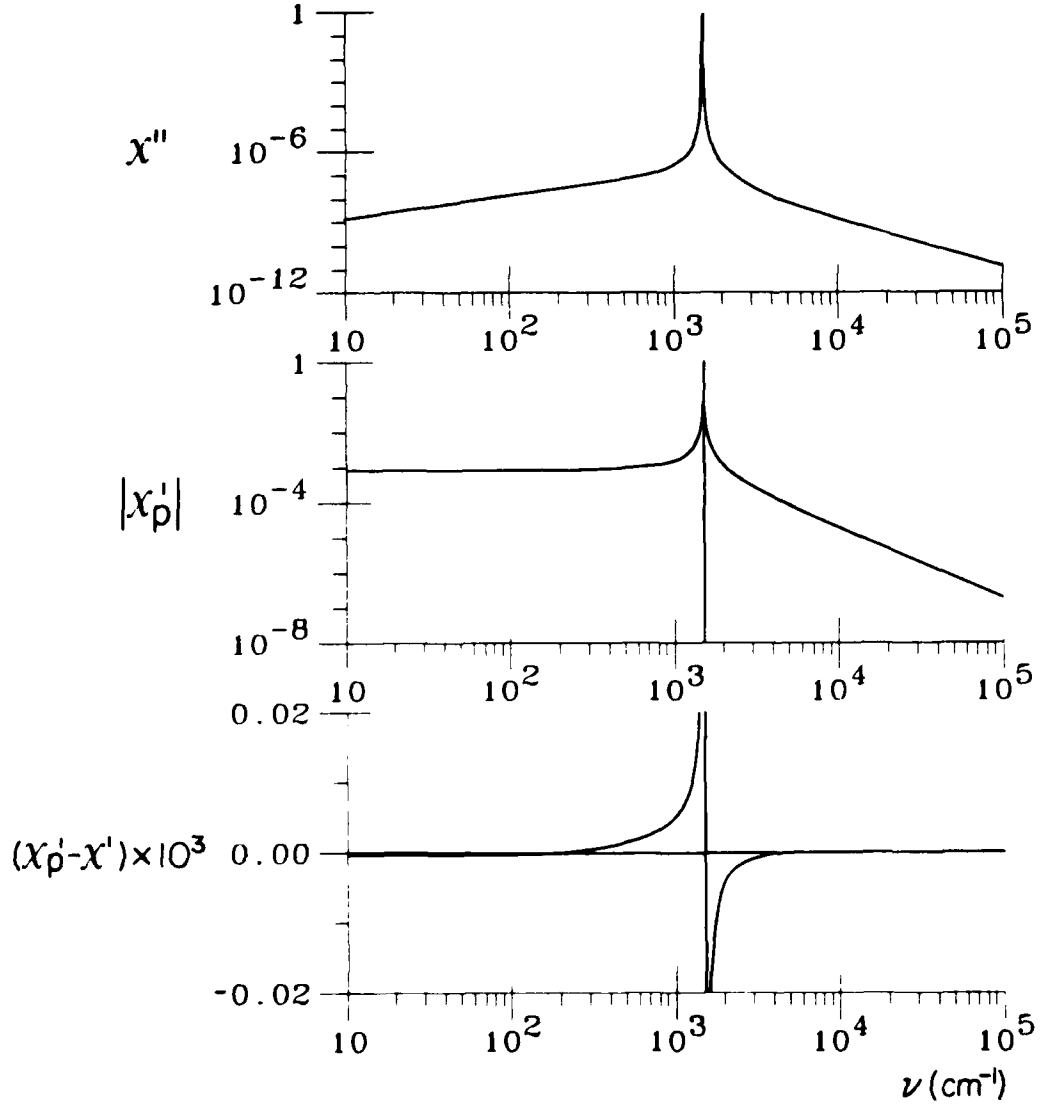

Figure 2C. Imaginary part of the susceptibility (χ''), magnitude of proposed real part of the susceptibility (χ'_p), and the difference between the proposed and actual real part ($\chi'_p - \chi'$) over an expanded spectral range for a single line with strength of 2 cm^{-1} at 1500 cm^{-1} and a halfwidth of 0.1 cm^{-1}

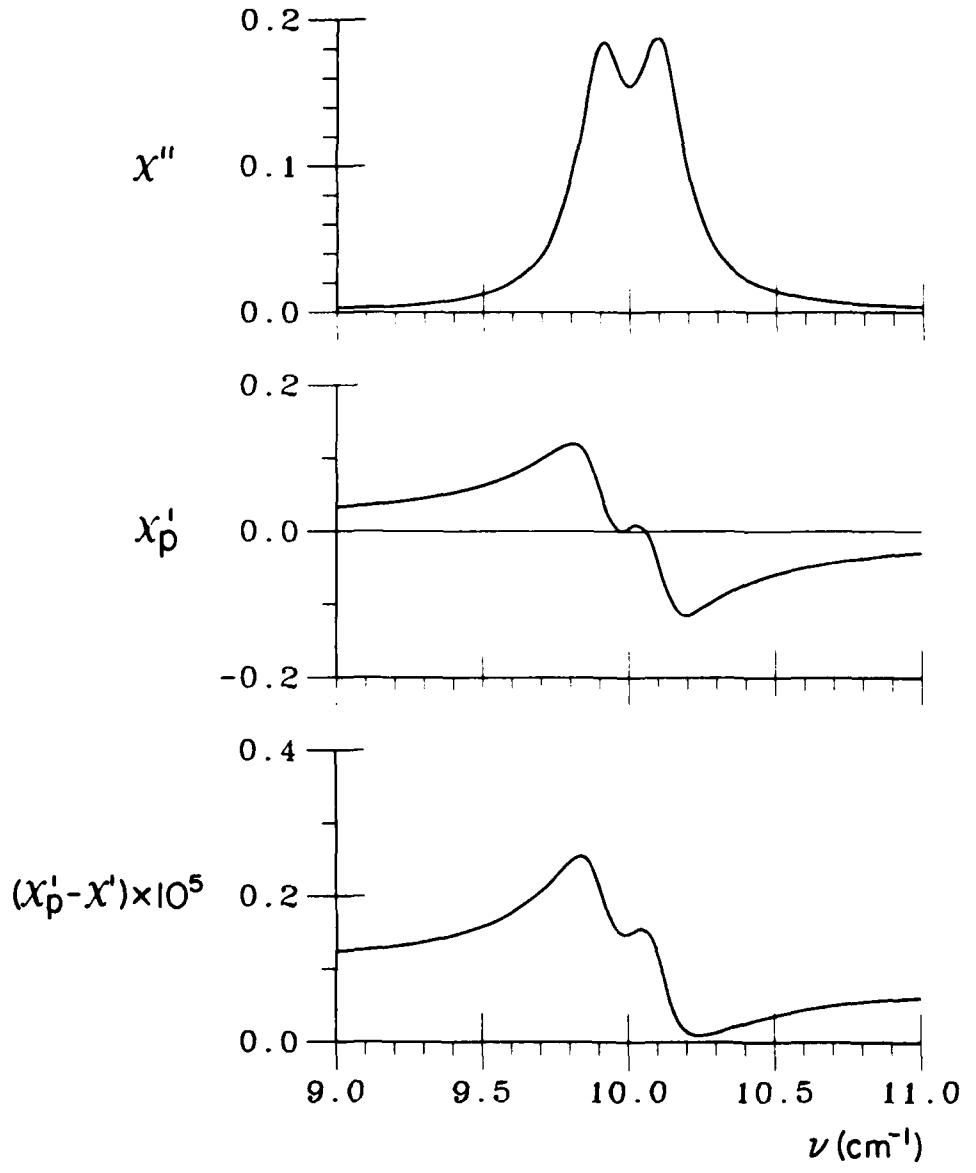

Figure 3A. Imaginary part of the susceptibility (χ''), proposed real part of the susceptibility (χ'_p), and the difference between the proposed and actual real part ($\chi'_p - \chi'$) as a function of wavenumber for two coupled lines of strength 2 cm^{-1} centered at 10 ±0.1 cm^{-1}, with halfwidths of 0.1 cm^{-1} and coupling coefficients of ±0.1 respectively

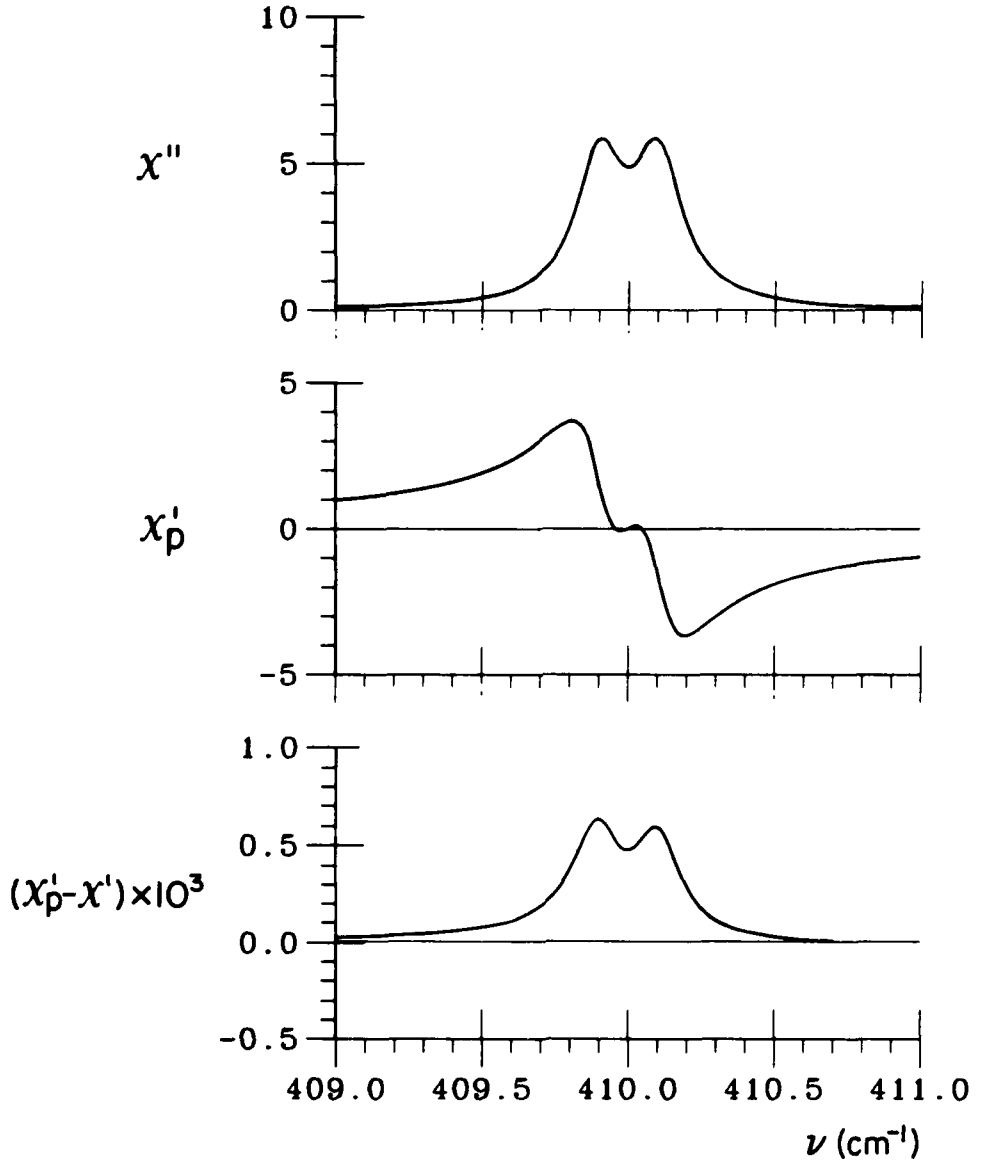

Figure 3B. Imaginary part of the susceptibility (χ''), proposed real part of the susceptibility (χ'_p), and the difference between the proposed and actual real part ($\chi'_p - \chi'$) as a function of wavenumber for two coupled lines of strength 2 cm^{-1} centered at 410 ±0.1 cm^{-1}, with halfwidths of 0.1 cm^{-1} and coupling coefficients of ±0.1 respectively

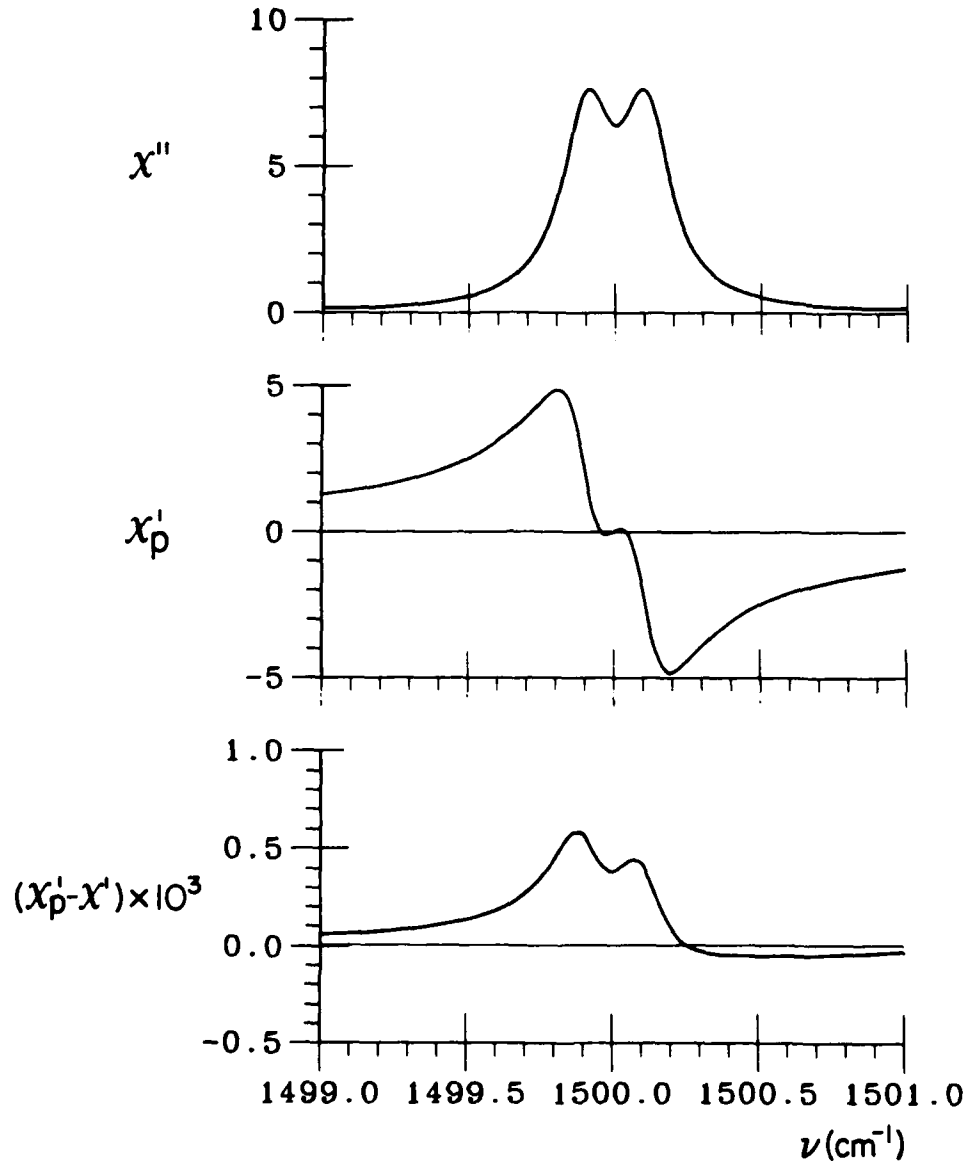

Figure 3C. Imaginary part of the susceptibility (χ "), proposed real part of the susceptibility (χ 'p), and the difference between the proposed and actual real part (χ 'p - χ ') as a function of wavenumber for two coupled lines of strength 2 cm^{-1} centered at 1500 ±0.1 cm^{-1}, with halfwidths of 0.1 cm^{-1} and coupling coefficients of ±0.1 respectively

Table 1. Summary of the Accuracy Test. The values in the parentheses are modified percent errors where a single extremum percent error at the zero crossing is eliminated from each case. Other values are S_i - 2.0, a_i - 0.1, y_1 = -0.1, y_2 = 0.1, b' = 1/412, and ϵ for the termination criterion is 10^{-6}

V_1(1/cm)	Range(1/cm)	Average Percent Error	No. of Iterations
Millimeter			
10.0	[9, 11]	0.002	50
	[0, 100]	0.42	50 - 51
	[0, 1500]	22	50 - 88
9.9 & 10.1	[9, 11]	0.004	50
	[0, 100]	0.46	50 - 51
	[0, 1500]	23	50 - 88
Intermediate			
410.0	[409, 411]	0.22(0.006)	68
	[0, 1910]	0.23(0.009)	62 - 116
409.9 & 410.1	[409, 411]	0.15	68
	[0, 1910]	0.11(0.010)	62 - 116
Infrared			
1500.0	[1499, 1501]	0.97(0.006)	177
	[0, 3000]	0.65(0.003)	136 - 213
1499.9 & 1500.1	[1499, 1501]	0.47(0.035)	177
	[0, 3000]	0.29(0.003)	177 - 213

consistency of the real and imaginary parts, has been the existence of a complete profile containing both positive and negative oscillators. Constant biases in these oscillators cancel each other and, therefore, the resulting function vanishes at infinity. The Hilbert transform of the resulting function is thus well-defined.

The effect of the line wing of the imaginary part on the Hilbert transform has been assessed using a profile composed of the difference of two Lorentz functions, for which the line wing decays as ν^{-4} instead of ν^{-2} for the simple Lorentz shape. The real part in the region far from line center, obtained from the modified profile, has been shown

to have the same asymptotic behavior as that of the simple Lorentz case. This demonstrates the decreased sensitivity of the Hilbert transform to the line wing of the imaginary part and supports the use of the impact line shape.

For evaluation of the validity of our approximate function, the Hilbert transform of the imaginary part of the susceptibility has been obtained in the form of an infinite series by exploiting the Lorentz expansion of the tanh(.) function and the known Hilbert transform of the Lorentz function. The resulting series has been successfully used in numerical verification of the proposed approximate real part. Excellent agreement has been demonstrated in the vicinity of the line center and generally good agreement over wider ranges. However, the gradual deterioration in the percentage accuracy far from line center in the millimeter case may be a significant problem for certain applications.

Several approaches could be considered to improve the validity of the proposed function. A fundamental reason for the error far from line center associated with the millimeter case is attributable to the inadequate approximation of the tanh(.) function over a broad spectral range. Consequently, for a broad spectral range it is expected that an improved approximation for the tanh(.) function would be required in order to obtain improved results. Alternatively, empirical corrections could be developed based on the functional characteristics of the error. Of particular significance would be the introduction of a small empirical shift in the line center to substantially reduce the percentage error in the line center region at which the real part of the susceptibility goes through zero.

Finally, it is noted that the proposed function can be used in conjunction with the line parameters over the entire frequency range. Thus the vast data base such as the line parameter compilation can be used for the evaluation of the real part of the susceptibility. The proposed function can be readily incorporated into line-by-line computational code.[24-26]

---

24. Clough, S.A., Kneizys, F.X., Rothman, L.S., and Gallery, W.O. (1981) Atmospheric spectral transmittance and radiance: FASCOD1B, SPIE Vol. 277-Atmospheric Transmission, pp 152-166.

25. Rothman, L.S., et al. (1983) AFGL trace gas compilation: 1982 version, Appl. Opt., 22, No. 11:1616-1627.

26. Rothman, L.S., et al. (1983) AFGL atmospheric absorption line parameters compilation: 1982 Edition, Appl. Opt., 22, No. 15:2247-2256.

References

1. Clough, S.A., Davis, R.W., and Tipping, R.H. (1983) The line shape for collisionally broadened molecular transitions: a quantum theory satisfying the fluctuation dissipation theorem, in Spectral Line Shape Vol. 2, edited by K. Burnett, Walter de Gruyter, New York, NY, 1983, pp 553-568.

2. Liebe, H.J. (1981) Modeling attenuation and phase of radio waves in air at frequencies below 1000 GHz, Radio Science, 16, No. 6:1183-1199.

3. Kemp, A.J., Birch, J.R., and Afsar, M.N. (1978) The refractive index of water vapor: a comparison of measurement and theory, Infrared Physics, 18:827-833.

4. Marshall, A.G., and Roe, D.C. (1978) Dispersion versus absorption: spectral line shape analysis for radiofrequency and microwave spectrometry, Analyt. Chem., 50, No. 6:756-763.

5. Kubo, R. The fluctuation-dissipation theorem, in Reports on Progress in Physics, Vol. XXIX Part 1, (1966), A.C. Stickland, Ed., The Institute of Physics and the Physical Society, London, pp 255-284.

6. Callen, H.B., and Welton, T.A., (1951) Irreversibility and generalized noise, Phys. Rev. 83:34-40.

7. Van Vleck, J.H., and Huber, D.L. (1977) Absorption, emission, and linebreadths: a semihistorical perspective, Rev. Mod. Phys. 49, No. 4:939-959.

8. Van Vleck, J.H., and Weisskopf, V.F. (1945) On the shape of collision-broadened lines, Rev. Mod. Phys. 17, Nos. 2 and 3:227-236.

9. Bolton, H.C. (1969) Some practical properties of Kronig-Kramers transforms, The Philosophical Magazine, 19, No. 159:487-499.

10. Fahrenfort, J. (1963) The methods and results of dispersion studies, Chapter XI in Infra-red Spectroscopy and Molecular Structure, M.M. Davies Ed., Elsevier, New York, NY.

11. Huber, D.L., and Van Vleck, J.H. (1966) The role of Boltzmann factors in line shape, Rev. Mod. Phys. 38, No. 1:187-204

12. Kramers, H.A. (1929) Die dispersion und absorption von Roentgenstrahlen, Physikalishe Zeitschrift, 30:522-523.

13. Kronig, R. de L, and Kramers, H.A. (1928) Absorption and dispersion in X-ray spectra, Z. Physik, 48, No. 3-4:174-179.

14. Kronig, R. de L. (1926) On the theory of dispersion of X-rays, J. Opt. Soc. Am. 12, No. 6:547-557.

15. Martin, P.C. (1967) Sum rules, Kramers-Kronig relations, and transport coefficients in charged systems, Phys. Rev., 161, No. 1:161-155.

16. Toll, J.S. (1956) Causality and the dispersion relation: logical foundations, Phys. Rev. 104, No. 6:1760-1770.

17. Townes, C.H., and Schwalow, A.L. (1955) Microwave Spectroscopy, McGraw-Hill Book Company, New York, NY.

18. Bateman Manuscript Project, (1954) Tables of Integral Transforms, Vols. 1 and 2, McGraw-Hill, New York, NY.

19. Baranger, M. (1958) Problem of overlapping lines in the theory of pressure broadening, Phys. Rev. 111, No. 2:494-504.

20. Rosenkranz, P.W. (1975) Shape of the 5 mm oxygen band in the atmosphere, IEEE Trans. Ant. Propagat., AP-23, No. 4:498-505.

21. Smith, E.W. (1981) Absorption and dispersion in the O_2 microwave spectrum at atmospheric pressures, J. Chem. Phys., 74:6658-6673.

22. Clough, S.A., Kneizys, F.X., Davis, R., Gamache, R., and Tipping, R. (1980) Theoretical line shape for H_2O vapor: application to the continuum, in Atmospheric Water Vapor, A. Deepak, T.D. Wilkerson, and L.H. Ruhnke, Eds., Academic Press, New York, NY, pp 25-46.

23. Gradshteyn, I.S. and Ryzhik, I.M. (1980) Table of Integrals, Series, and Products A. Jeffrey Trans., Academic Press, New York, NY.

24. Clough, S.A., Kneizys, F.X., Rothman, L.S., and Gallery, W.O. (1981) Atmospheric spectral transmittance and radiance: FASCOD1B, SPIE Vol. 277-Atmospheric Transmission, pp 152-166.

25. Rothman, L.S., et al. (1983) AFGL trace gas compilation: 1982 version, Appl. Opt., 22, No. 11:1616-1627.

26. Rothman, L.S., et al. (1983) AFGL atmospheric absorption line parameters compilation: 1982 Edition, Appl. Opt., 22, No. 15:2247-2256.

A1. Abraham, M. and Becker, R. (1949) The Classical Theory of Electricity and Magnetism, Hafner Publishing Company, New York, NY.

B1. Brown, D.R. (1984) Dispersion profiles for near millimeter wave oxygen refractivity, Private communication.

B2. Bracewell, R.N. (1978) The Fourier Transform and Its Applications, Second Edition, McGraw-Hill, New York, NY.

Appendix A

Summary of Classical Relations

In this appendix, a summary of the classical relationships among the susceptibility, dielectric constant, and index of refraction are presented. The definitions of the parameters and the derivation of the wave equation follow Abraham and Becker.[A1]

For a homogeneous, isotropic dielectric in which the current density and charge density have been assumed to be zero, Maxwell's equations are

$$\bar{\nabla} \times \bar{H} = \frac{1}{c} \frac{\partial \bar{D}}{\partial t} , \tag{A1}$$

$$\bar{\nabla} \times \bar{E} = -\frac{1}{c} \frac{\partial \bar{B}}{\partial t} , \tag{A2}$$

$$\bar{\nabla} \cdot \bar{D} = 0, \tag{A3}$$

$$\bar{\nabla} \cdot \bar{B} = 0, \tag{A4}$$

where

$\bar{H}$ = magnetic field strength
$\bar{E}$ = electric field strength
$\bar{D}$ = dielectric displacement
$\bar{B}$ = magnetic induction

and c is the velocity of light.

We also have the further definitions, for non-ferromagnetic substances, following Abraham and Becker[A1] that

$$\bar{D} = \bar{E} + 4 \pi \bar{P}, \tag{A5}$$

where P is the dielectric polarization and that

$$\bar{D} = \epsilon \bar{E}, \tag{A6}$$

$$\bar{B} = \mu \bar{H}, \tag{A7}$$

$$\bar{P} = \chi \bar{E}, \tag{A8}$$

A1. Abraham, M. and Becker, R. (1949) The Classical Theory of Electricity and Magnetism, Hafner Publishing Company, New York, NY.

with

ϵ = dielectric constant

μ = permeability

χ = dielectric susceptibility

Substituting Eqs. (A6) and (A8) into Eq. (A5), and neglecting any internal electric fields gives

$$\epsilon = 1 + 4\pi\chi . \tag{A9}$$

As shown in Abraham and Becker,[A1] the wave equation, derived from Maxwell's equations and Eqs. (A6) and (A7), is given by

$$\nabla^2 \vec{E} = \frac{\mu\epsilon}{c^2} \frac{\partial^2 \vec{E}}{\partial t^2} , \tag{A10}$$

with a similar equation for the magnetic field strength H.

The velocity of propagation of the electromagnetic wave, v, is defined as

$$v = c / \sqrt{\mu\epsilon} , \tag{A11}$$

and the refractive index of the medium, n, as

$$n^2 = (c/v)^2 = \mu\epsilon . \tag{A12}$$

For materials with, $\mu \simeq 1$, Eq. (A12) becomes

$$n^2 = \epsilon , \tag{A13}$$

and we have, by combining Eqs. (A9) and (A13)

$$4\pi\chi = n^2 - 1, \tag{A14}$$

with n, ϵ, and χ real.

For a plane wave of amplitude E_0 and wavenumber value $\nu = \omega/2\pi c$, propagating in the z-direction, the solution to Eq. (A10) is

$$E_x = E_0 \exp[i2\pi\nu(ct - nz)], \tag{A15}$$

with $E_z = E_y = 0$, and a similar equation for the magnetic field H_y of amplitude H_0

$$H_y = H_0 \exp[i2\pi\nu(ct - nz)], \tag{A16}$$

with $H_x = H_z = 0$. Substituting Eqs. (A15) and (A16) into Eq. (A2) gives the relationship between the field amplitudes.

$$H_0 = \frac{n}{\mu} E_0. \tag{A17}$$

The energy transport per unit area per unit time is given by the Poynting vector N, defined by

$$\overline{N} = \frac{c}{4\pi} (\overline{E} \times \overline{H}), \tag{A18}$$

and for the plane wave solution, the cycle averaged component of the Poynting vector is

$$< N_z > = \frac{1}{2}\left(\frac{c}{4\pi}\right)\left(\frac{n}{\mu}\right) E_0^2. \tag{A19}$$

For the general case where the dielectric constant is complex, that is

$$\epsilon = \epsilon' - i\epsilon'', \tag{A20}$$

the index of refraction and the susceptibility also become complex and are defined as

$$n = n' - i n'', \tag{A21}$$

$$\chi = \chi' - i\chi''. \tag{A22}$$

Equation (A12) is still valid with the complex quantities, and the plane wave solution is

$$E_x = E_0 \exp[i2\pi\nu(ct - nz)]$$

$$= E_0 \exp[-2\pi n''\nu z] \exp[i2\pi\nu(ct - n'z)], \tag{A23}$$

for the electric vector, and

$$H_y = H_0 \exp[-2\pi n'' \nu z] \exp[i2\pi\nu (ct - n'z)], \tag{A24}$$

for the magnetic vector, with

$$H_0 = \frac{n}{\mu} E_0 = \frac{n'-in''}{\mu} E_0. \tag{A25}$$

An alternate form of Eq. (A25) explicitly in terms of the phase angle between the electric and magnetic amplitudes is given by

$$H_0 = \frac{|n|}{\mu} e^{-i\phi} E_0, \tag{A26}$$

where $\tan \phi = n''/n'$ and $|n| = [n'^2+n''^2]^{1/2}$.

If $\mu \simeq 1$, Eq. (A13) can be written explicitly in terms of its real and imaginary parts

$$(n' - i\, n'')^2 = \epsilon' - i\, \epsilon'', \tag{A27}$$

or

$$\epsilon' = n'^2 - n''^2, \tag{A28}$$

$$\epsilon'' = 2\, n'n''. \tag{A29}$$

From Eqs. (A9) and (A29), for the susceptibility we obtain

$$4\pi X' = n'^2 - 1 - n''^2, \tag{A30}$$

$$4\pi X'' = 2n'n''. \tag{A31}$$

For a complex index of refraction and dielectric constant, Eqs. (A23) and (A24) are damped plane wave solutions with the real part of the cycle averaged Poynting vector given by

$$< N_z > = \frac{1}{2} \left(\frac{c}{4\pi}\right) \left(\frac{n'}{\mu}\right) E_0^2 \exp\left[-4\pi n'' \nu z\right], \tag{A32}$$

which defines an absorption coefficient, κ, as

$$\kappa = 4\pi n'' \nu. \tag{A33}$$

Appendix B

Hilbert Transform of Lorentz Type Functions

We consider the Hilbert transform of the following two Lorentz type functions that appear repeatedly in the main body of this report. We note that this appendix follows Brown[B1] closely.

$$f(\nu) = \frac{(\alpha/\pi)}{[(\nu - \nu_0)^2 + \alpha^2]}. \tag{B1}$$

$$g(\nu) = \frac{[(\nu - \nu_0)/\pi]}{[(\nu - \nu_0)^2 + \alpha^2]}. \tag{B2}$$

The Hilbert transform of functions $f(-\nu)$ and $g(-\nu)$ which also appear in the text can be obtained from those of the above functions as shown later.

Consider the Hilbert transform $F(\nu)$ of (B1) first.

$$F(\nu) = (1/\pi) \int_{-\infty}^{\infty} \frac{(\alpha/\pi)}{[(u - \nu)\ (u - \nu_0)^2 + \alpha^2\ ]}\, du. \tag{B3}$$

Using the change of variable

$$t = \frac{(u - \nu_0)}{\alpha}, \tag{B4}$$

we can rewrite the integral in Eq. (B3) as

$$F(\nu) = (1/\pi^2\alpha) \int_{-\infty}^{\infty} \frac{1}{[(t - x)\ (t^2 + 1)]}\, dt, \tag{B5}$$

where $x = (\nu - \nu_0)/\alpha$. The Cauchy principal value of the integral in Eq. (B5) can be obtained by expanding the integrand using the partial fraction as

---

B1. Brown, D.R. (1984) Dispersion profiles for near millimeter wave oxygen refractivity, Private communication.

$$F(\nu) = \frac{1}{[\pi^2 \alpha (x^2+1)]} \int_{-\infty}^{\infty} [\frac{1}{(t-x)} - \frac{t}{(t^2+1)} - \frac{x}{(t^2+1)}] \, dt$$

$$= \frac{-x}{[\pi \alpha (x^2 + 1)]} = -g(\nu). \tag{B6}$$

On the other hand, the change of the dummy variable in the definition of the Hilbert transform from u to -u gives us the following property for a general function ϕ.

$$H[\phi(-\nu)] = - H[\phi(\nu)]: \; _{\nu \to -\nu}. \tag{B7}$$

Therefore the Hilbert transform of $f(-\nu)$ is

$$H[f(-\nu)] = - F(-\nu) = g(-\nu). \tag{B8}$$

For $H[g(\nu)]$, we may either use the symmetry of the Hilbert transform[B2] and the above result or follow a similar derivation. Here we will go through the latter path. After the same change of variable, we arrive at

$$G(\nu) = H[g(\nu)]$$

$$= (1/\pi^2 \alpha) \int_{-\infty}^{\infty} \frac{t}{[(t - x)(t^2 + 1)]} \, dt, \tag{B9}$$

where x is defined above. Following the $F(\nu)$ case, we have

$$G(\nu) = \frac{1}{[\pi^2 \alpha (x^2+1)]} \int_{-\infty}^{\infty} [\frac{x}{(t-x)} - \frac{xt}{(t^2+1)} + \frac{1}{(t^2+1)}] \, dt$$

$$= \frac{1}{[\pi \alpha (x^2 + 1)]} = f(\nu). \tag{B10}$$

B2. Bracewell, R.N. (1978) The Fourier Transform and Its Applications, Second Edition, McGraw-Hill, New York, NY.

From this the $g(-\nu)$ case can easily be obtained as

$$H[g(-\nu)] = - G(-\nu) = - f(-\nu). \qquad \text{(B11)}$$

☆ U. S. GOVERNMENT PRINTING OFFICE: 1987--700-000--30,027

END

8-87

DTIC